

No. 33

**REPORT
ON
THE MINERAL EXPLORATION
IN
VANUA LEVU
THE REPUBLIC OF FIJI
CONSOLIDATED REPORT**

FEBRUARY 1998

JICA LIBRARY



J 1141622 (9)

**JAPAN INTERNATIONAL COOPERATION AGENCY
METAL MINING AGENCY OF JAPAN**

MPN

J R

98-046

**REPORT
ON
THE MINERAL EXPLORATION
IN
VANUA LEVU
THE REPUBLIC OF FIJI
CONSOLIDATED REPORT**

FEBRUARY 1998

**JAPAN INTERNATIONAL COOPERATION AGENCY
METAL MINING AGENCY OF JAPAN**



1141622 {9}

PREFACE

In response to the request by the Government of the Republic of Fiji, the Japanese Government decided to conduct a mineral exploration project in Vanua Levu and entrusted the survey to the Japan International Cooperation Agency (JICA) and the Metal Mining Agency of Japan (MMAJ).

The survey has been conducted jointly by experts of both Governments. The collaboration survey for metallic mineral, which lasted three years, consisted of geological, geochemical, geophysical surveys and exploration drilling supported by laboratory work. The team exchanged views with the officials concerned with the Government of the Republic of Fiji and conducted a field survey in Vanua Levu. This consolidated report hereby submitted summarizes results of the said survey.

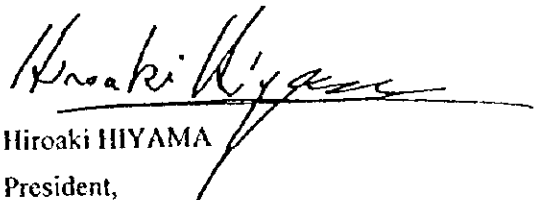
We hope that this report will be useful for the development of the Republic of Fiji and contribute to the promotion of friendly relations between our two countries.

We wish to express our deep appreciation to the officials concerned of the Government of the Republic of Fiji for close cooperation extended to the Japanese team.

February 1998



Kimio Fujita
President,
Japan International Cooperation Agency



Hiroaki HIYAMA
President,
Metal Mining Agency of Japan

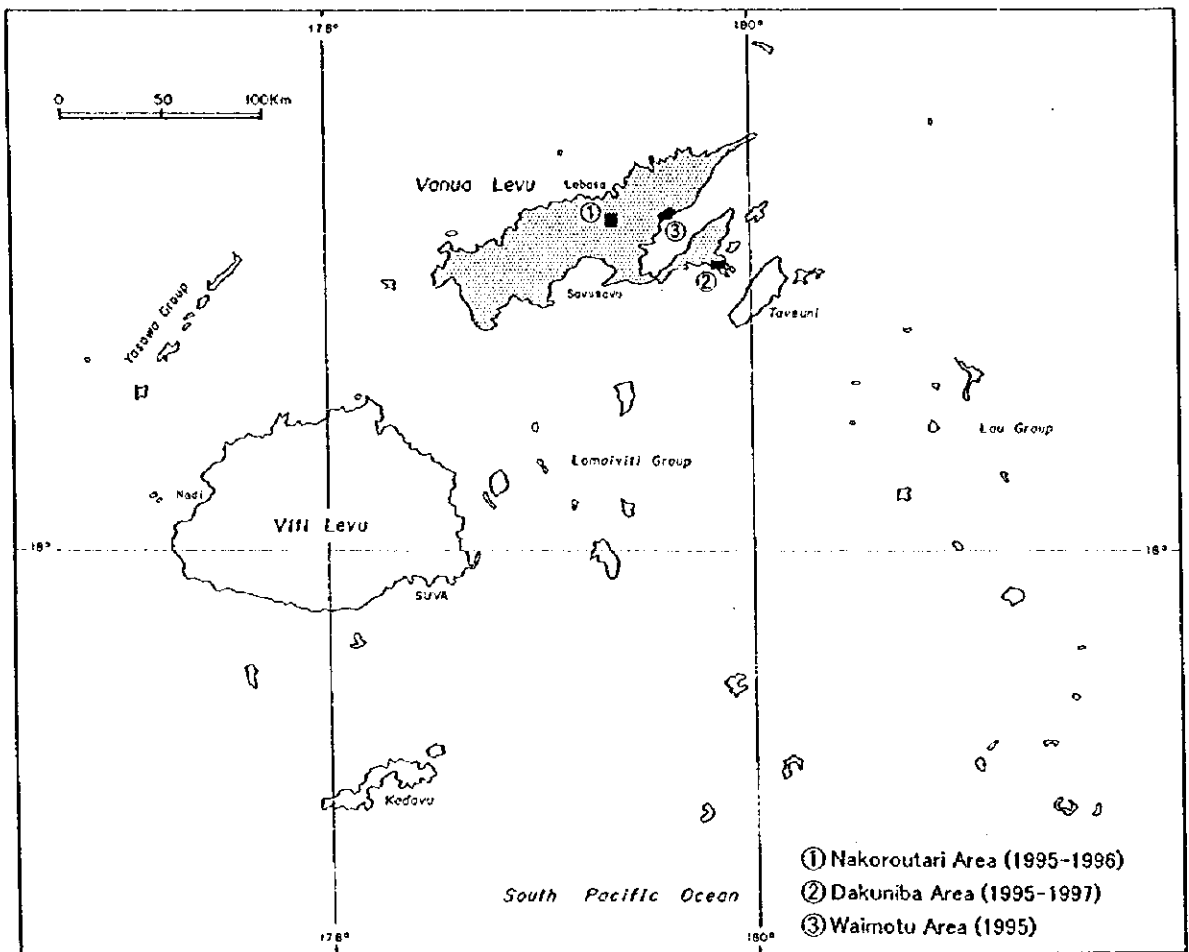
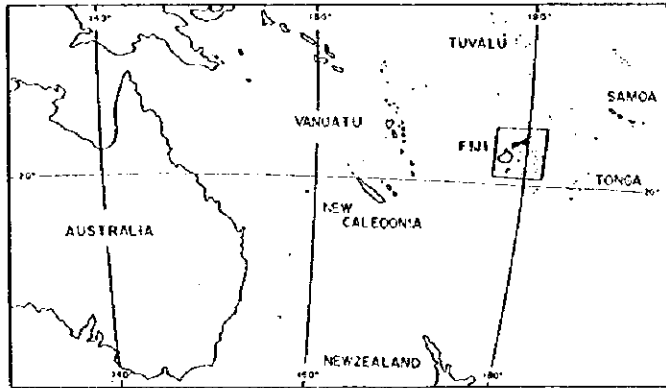


Fig. 1-1 Index Map of the Survey Area

SUMMARY

Mineral Exploration was carried out in the Vanua Levu Island of the Republic of Fiji during the period of three years from 1995 to 1997. The objective of the project was to assess the mineral potential of the area by geological survey, geochemical survey, geophysical survey and drilling.

During the first-phase of the Vanua Levu mineral exploration project; three promising areas (100 km²), namely Nakoroutari, Dakuniba, and Waimotu were delineated by analysis and interpretation of existing geological and mineral resources data and information of the island (5,500km²). Geological and geochemical surveys were carried out in these three areas and Array CSAMT and time-domain IP surveys were made in the Nakoroutari. Several promising zones were extracted in these areas. Then, the second phase comprised drilling of both three localities within the Nakoroutari area and the Dakuniba Area, respectively. Finally, the third phase comprised drilling of three localities within the Dakuniba Area.

(1) Nakoroutari Area

The geology of Nakoroutari Area is composed mainly of basalt-andesite lava and volcanics of the Koroutari Andesites and andesitic volcanics of the Sueni Breccias, which belong to Upper Miocene-Lower Pliocene Natewa Volcanic Group. Mineralization and alteration were observed at five zones; namely Leli's Prospect, a locality to the south of the same Prospect, Navakuru, Mugsy's Prospect and a locality to the east of the Mugsy's Prospect. Leli's Prospect is the most promising of the above and also the altered zone to the south of Leli's show evidences of gold mineralization. At Leli's Prospect, two quartz veins were observed within a brecciated zone and the highest grade is 12.9 g/tAu.

In the vicinity of Leli's Prospect, array CSAMT was carried out for 12 km and time domain IP for 7.5 km. A high resistivity body was detected by CSAMT in the central part, and this is inferred to consist of two buried silicified zones elongated in the N-S direction, and the whole altered zone was found to extend in the NW-SE direction. A weak chargeability anomaly extending in the NW-SE direction was detected by IP, but anomalies over wide areal extent were not detected.

Drilling in this area (MJFV-1, -2, -3) confirmed the ores would extend 600 m in the strike direction (NNW-SSE). Judging from the widths and gold grades of the veins that drill holes encountered, however, it is not felt that promising gold deposits are emplaced in this area. No further work in this area is recommended.

(2) Dakuniba Area

Mineralization of the Dakuniba Area consists of quartz veins developed in basaltic lava and basaltic volcanoclastic rocks which belong to the Dakuniba Basalt of the Natewa Volcanic Group. The major

quartz veins are exposed in the upper reaches of the Nagagani Creek in the central part of the area. The veins strike in the WNW-ESE direction with steep S or N dip and the total length exceeds 2km. Alteration zones associated with mineralization were observed in the northeastern part of the area. They are quartz-clay veins extending from the upper reaches of Wailevu Creek to Nagagani Creek, argillized and pyrite dissemination from the Nubuni Creek westward, and mineralization observed in the quartz veins near a tributary of the Waikava Creek.

The continuity of individual quartz veins exposed in the upper reaches of the Nagagani Creek had not been confirmed by surface traversing. The grade of the quartz veins, however, high with a maximum of 16g/tAu and 21 samples containing more than 1g/tAu were collected from a zone of only 1km length. Thus this zone was considered to be a promising prospect.

Then, a total of 2,000 m length by six holes was drilled during the second and third years. Three holes drilled during the second year, namely MJFV-4, -5, and -6, all encountered quartz veins and clay veins containing quartz-silicified angular fragments. Each hole encountered veins and several mineralized zones at depth inferred from the investigation of surface outcrops and trenches. Then, all three holes drilled during the third year, namely MJFV-7, -8, and -9, confirmed argillized zone accompanied by silicified breccia. The existence of this zone in these drill holes was inferred from the results of the drilling at MJFV-4, -5, and -6. The drilling result of each hole is summarized as follows.

- Particularly the hole MJFV-5 confirmed the existence of a clay vein with a high average gold content of 11.3 g/t in a width of 2.2 m, and 0.60 m within this vein contained an average of 27.6 g/tAu, the highest assay result of this area. This vein contains angular fragments of quartz and silicified rocks. In this MJFV-5, existence of five zones containing higher than 1 g/tAu was confirmed within an interval of approximately 60 m below this high-gold vein. This indicates stronger mineralization in the subsurface zones compared to the surface showings.
- The hole MJFV-4 confirmed mineralized zones at three depths, two of which are clay veins containing silicified fragments, and the other a silicified-argillized zone accompanied by quartz veins. The maximum gold content of these zones is 0.79 g/tAu (0.30 m width), and although it is weaker than the surface showings, continuation of gold mineralization into the deeper parts was confirmed.
- In the hole MJFV-6, there are many quartz veins between 55 m and 129 m depth, and alteration accompanied by chlorite-mixed layer minerals occurs extensively near the bottom of the targeted trench. In the deeper parts, chlorite alteration occurs extensively which is accompanied by disseminated to irregular vein pyrite. The highest assay result is 0.2 g/tAu and lower than the surface showings.
- The hole MJFV-7 penetrated argillized zone with quartz breccia-silicified breccia at; 226.60-228.00 m

depth (1.40 m thick), 249.90-253.70 m depth (3.80 m thick), and 259.10-260.20 m depth (1.10 m thick). The grade was 0.41g/tAu, 0.47g/tAu, and 0.27g/tAu respectively. Of the above gold-bearing horizons, the grade at 227.50-227.60 m (0.10 m thick) and 251.05-251.20 m depths (0.15 m thick) was 2.3g/tAu and 3.1g/tAu respectively, exceeding 1g/tAu.

- The hole MJFV-8 confirmed the existence of the mineralized zone at three horizons. The zone encountered at 116.80-130.30 m depth (13.50 m thick) was a clay vein including a silicified zone and the grade was 0.23g/tAu, 0.55g/tAu, 0.64g/tAu, 0.32g/tAu, 0.63g/tAu, and 1.9g/tAu at depths of 116.80-117.25 m (0.45 m thick), 118.10-118.60 m (0.50 m thick), 122.10-123.80 m (1.70 m thick), 124.30-124.70 m (0.40 m thick), 125.10-127.70 m (2.60 m thick), and 128.15-129.25 m (1.10 m thick) respectively. Both the altered zones at 141.45-141.70 m (0.25 m thick) and 142.60-143.00 m depths (0.40 m thick) contained 0.47g/tAu. The gold content of the silicified zone at 279.90-280.70 m depth (0.80 m thick) was less than 0.08g/tAu.
- In the hole MJFV-9, there are many quartz-calcite veins between 87.20-93.35 m depth, and gold content of 1.01g/tAu, 0.46g/tAu, and 0.34g/tAu was confirmed at 87.20-87.30 m (0.10 m thick), 88.10-88.45 m (0.35 m thick), and 90.70-94.75 m (4.05 m thick) respectively. The interval of 93.75-94.05 m (0.30 m thick) showed particularly high gold content of 2.3 g/tAu, the highest value of MJFV-9.

The major ore zones encountered by the three MJFV-7, -8 and -9 drill holes; namely the three zones between 226.60 m-260.20 m depth of MJFV-7, silicified argillized zone at 116.80-130.30 m depth of MJFV-8, and the quartz-calcite veinlet zone at 87.20-95.35 m depth of MJFV-9 were confirmed to be continuous to the quartz breccia-bearing silicified breccia clay zone encountered in MJFV-5 with a WNW-ESE strike. Thus, the continuity of the mineralized zone inferred from the results of the second year survey to exist for 700 m from MJFV-4 to -6 was confirmed in the subsurface part of the area in the third year survey.

Although the assay results of these cores are lower than that of MJFV-5, the grade distribution agrees with the general eastward dip. This mineralized zone extends further east and westward, but its surface showings are weak.

The distribution of altered minerals clarified by the results of studies regarding; gold grade distribution, fluid inclusion data, and X-ray diffraction data reported above alone is not sufficient for inferring the mineral prospectivity in the lower subsurface zone of the area. Also the mineral potential of other areas is difficult to consider since only surface data are available. However, since widespread gold mineralization was confirmed in the Nagagani Creek area, it is believed that other parts of the Dakuniba Area has sufficient mineral potential for further exploration.

(3) Waimotu Area

There are three prospects in this area; namely Waimotu Lodes, Bill's Hill Prospect, and Nuku Prospect. The orebodies and mineralization occur in weakly propylitized andesite-basalt lava and basaltic volcaniclastic rocks.

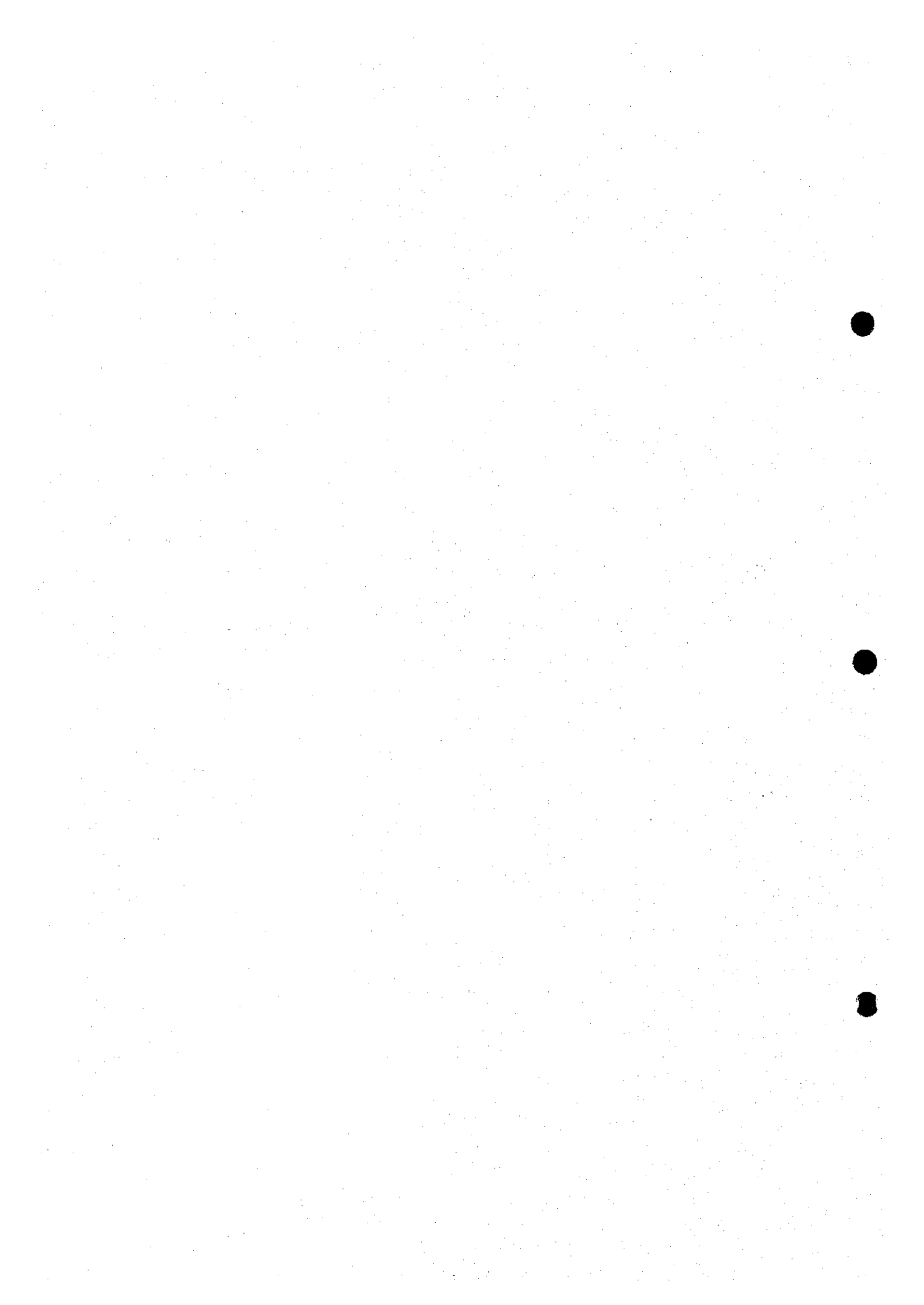
The Waimotu Lodes are comprised of; Main Lode, East Lode, and West Lode. These are chalcedony and quartz veins extending in the N-S direction and the maximum gold grades obtained during the first year survey are; Main Lode 24 g/tAu (1.0 m wide), East Lode 43 g/tAu (0.8 m wide), West Lode 0.92 g/t (boulder). The northern and southern extensions of the Waimotu Lodes are not exposed well and the mineralization and alteration have not been confirmed.

At Bill's Hill, silicified, argillized, and pyrite-disseminated layers are developed. Quartz and chalcedony stockwork are developed cutting through the altered zone with mostly N-S strike and steep dip. Assay of all samples collected showed gold content of less than 1 g/tAu.

At Nuku, the extension of a silicified zone associated with chalcedony and quartz veins was confirmed for 150 m. It is believed that this zone strikes in the N-S direction with steep westward dip. The maximum assay result of the collected samples is 4.3 g/tAu (sampled width 2.5 m) and the average value was 1.3 g/tAu (average vein width 7 m). The grade of the cores of previous drilling at shallow zones is 0.6 g/tAu (ore width 7 m).

In the past, geological survey and exploration were carried out covering limited parts of the Waimotu Lodes, Bill's Hill, and Nuku Prospects. This work, however, is not sufficient for assessment of the resources in the area. Of these three zones, the Waimotu Lode has the highest assay results from outcrop and is therefore most interesting. Therefore, it is recommended that we first confirm the downward continuity and the distribution of the veins by geophysical survey, namely CSAMT and IP, then follow it up by drilling.

CONTENTS



CONTENTS

PREFACE

MAP OF THE SURVEY AREA

SUMMARY

CONTENTS i

LIST OF FIGURES AND TABLES v

PART I OVERVIEW 1

Chapter 1 Introduction 1

1-1 Background and Objectives 1

1-2 Survey Methods 2

1-3 Duration of Survey and Participants 3

Chapter 2 Outline of Past Geological Surveys 4

Chapter 3 Geography of the Project Area 5

3-1 Location and Access 5

3-2 Topography 5

3-3 Climate and Vegetation 5

Chapter 4 General Geology of the Survey Area 6

4-1 Geologic Setting: Plate Tectonics 6

4-2 Geologic Setting of the Survey Area 7

4-3 Brief History of Mining in the Survey Area 7

Chapter 5 Conclusions and Recommendations 9

5-1 Conclusions 9

5-1-1 Nakoroutari Area 9

5-1-2 Dakuniba Area 11

5-1-3 Waimotu Area 13

5-2 Recommendations 14

5-2-1 Nakoroutari area 14

5-2-2 Dakuniba Area 14

5-2-3 Waimotu Area	15
--------------------------	----

PART II DETAILED DISCUSSIONS 37

Chapter 1 Compilation of Existing Data	37
1-1 Survey Method	37
1-2 SLAR Imagery Interpretation	37
1-2-1 Outline	37
1-2-2 Interpretation of Geological Structure	39
1-2-3 Interpretation of the Geological Structure	40
1-3 Selection of Geological Survey Areas	41
1-3-1 Outline	41
1-3-2 Nakoroutari Area	42
1-3-3 Dakuniba Area	43
1-3-4 Waimotu Area	44
Chapter 2 Nakoroutari Area	46
2-1 Geological Survey	46
2-1-1 General Geology	46
2-1-2 Stratigraphy	46
2-1-3 Intrusive Rocks	47
2-1-4 Geologic Structure	47
2-1-5 Mineralization and Alteration	48
2-2 Geochemical Survey	49
2-2-1 Method	49
2-2-2 Assay results and Basic Statistic Data	49
2-3 Geophysical Survey (Array CSAMT and Time Domain IP Methods)	50
2-3-1 Outline of Geophysical Survey	50
2-3-3 Time Domain IP Method	54
2-3-4 Results of Array CSAMT Method	55
2-3-5 Results of Time Domain IP method	57
2-3-6 Laboratory Investigations	61
2-3-7 Summary of Geophysical Survey and Discussions	62
2-4 Drilling	64
2-4-1 Method	64
2-4-2 Drilling Method	64

2-4-3	Geology, Mineralization and Alteration	65
2-4-4	Considerations on the Nakoroutari Area	72
Chapter 3	Dakuniba Area	75
3-1	Geological Survey	75
3-1-1	Outline of Geology	75
3-1-2	Stratigraphy	75
3-1-3	Intrusive Rocks	75
3-1-4	Geologic Structure	76
3-1-5	Mineralization and Alteration	76
3-2	Geochemical Survey	76
3-2-1	Method and Results	76
3-2-2	Correlation	78
3-2-3	Considerations	78
3-3	Drilling	78
3-3-1	Location and Lengths	78
3-3-2	Method	79
3-3-3	Geology, Alteration and Mineralization	79
3-3-4	Summary of Drilling Results and Considerations	97
Chapter 4	Waimotu Area	101
4-1	Geological Survey	101
4-1-1	General Geology	101
4-1-2	Stratigraphy	101
4-1-3	Intrusive Rocks	102
4-1-4	Geological Structure	102
4-1-5	Mineralization and Alteration	103
4-2	Geochemical Survey	103
4-2-1	Samples and Basic Statistics	103
4-2-2	Correlation	104
4-3	Considerations	105
PART III	CONCLUSIONS AND RECOMMENDATIONS	289
Chapter 1	Nakoroutari Area	289
1-1	Conclusions	289
1-2	Recommendations	290

Chapter 2 Dakuniba Area	291
2-1 Conclusions	291
2-2 Recommendations	293
Chapter 3 Waimotu Area	294
3-1 Conclusions	294
3-2 Recommendations	295
REFERENCES	297
APPENDIX	

LIST OF FIGURES AND TABLES

FIGURES

- Fig. 1-1 Index Map of the Survey Area
- Fig. 1-2 Flow-sheet of the Survey
- Fig. 1-3 Location Map of the Survey Area
- Fig. 1-4 Simplified Geologic Map around the Survey Area
- Fig. 1-5 Integrated Interpretation Map of Data Compilation Area
- Fig. 1-6 Integrated Map of the Nakoroutari Area
- Fig. 1-7 Survey Results of the Nakoroutari Area
- Fig. 1-8 Detailed Survey Results of the Leli's Prospect
- Fig. 1-9 Geologic Map of the Dakuniba Area
- Fig. 1-10 Integrated Map of the Dakuniba Area
- Fig. 1-11 Survey Results of the Dakuniba Area
- Fig. 1-12 Geologic Map of the Waimotu Area
- Fig. 1-13 Integrated Map of the Waimotu Area
-
- Fig. 2-1-1 SLAR Imagery Mosaic of Vanua Levu
- Fig. 2-1-2 Photogeological Interpretation Map Using SLAR Imagery of Vanua Levu
- Fig. 2-1-3 Rose Diagrams of Number and Length, and Histogram of Length of Lineaments
Interpreted from SLAR Imagery of Vanua Levu
- Fig. 2-1-4 Tectonic Interpretation Map of SLAR Imagery
- Fig. 2-1-5 Location Map of the Nakoroutari Area
- Fig. 2-1-6 Location Map of the Dakuniba Area
- Fig. 2-1-7 Location Map of the Waimotu Area
- Fig. 2-2-1 Schematic Stratigraphic Columns of the Nakoroutari Area
- Fig. 2-2-2 Sample Location Map of the Nakoroutari Area
- Fig. 2-2-3 Summary Map of Existing Data of the Nakoroutari Area
- Fig. 2-2-4 Distribution Map of Prospects and Alteration Zones in the Nakoroutari Area
- Fig. 2-2-5 Detailed Survey Results of the Leli's Prospect
- Fig. 2-2-6 Histogram of Assay Values(the Nakoroutari Area)
- Fig. 2-2-7 Cumulative Frequency Distribution of Assay Values (the Nakoroutari Area)
- Fig. 2-2-8 Correlation between Elements (the Nakoroutari Area)
- Fig. 2-2-9 Geochemical Survey Results of the Nakoroutari Area

- Fig. 2-2-10 Geochemical Survey Results of the Leli's Prospect Area
- Fig. 2-2-11 Location Map of Survey Area and Transmitting Dipole
- Fig. 2-2-12 Location Map of Survey Lines
- Fig. 2-2-13 Survey Configuration of CSAMT Method
- Fig. 2-2-14 Flow Chart of 1-d. Automatic Interpretation for CSAMT Data
- Fig. 2-2-15 Survey Configuration of IP Method
- Fig. 2-2-16 (1) CSAMT Pseudo-section of Apparent Resistivity [Line A-D]
- Fig. 2-2-16 (2) CSAMT Pseudo-section of Apparent Resistivity [Line E-H]
- Fig. 2-2-17 (1) CSAMT Plane Map of Apparent Resistivity [2,048Hz]
- Fig. 2-2-17 (2) CSAMT Plane Map of Apparent Resistivity [256Hz]
- Fig. 2-2-17 (3) CSAMT Plane Map of Apparent Resistivity [32Hz]
- Fig. 2-2-18 (1) CSAMT 2-d. Simulation Analysis [Line A-D]
- Fig. 2-2-18 (2) CSAMT 2-d. Simulation Analysis [Line E-H]
- Fig. 2-2-19 CSAMT Interpretation Map
- Fig. 2-2-20 TDIP Pseudo-section of Apparent Resistivity [Line B-F]
- Fig. 2-2-21 (1) TDIP Plane Map of Apparent Resistivity [n=1]
- Fig. 2-2-21 (2) TDIP Plane Map of Apparent Resistivity [n=2]
- Fig. 2-2-21 (3) TDIP Plane Map of Apparent Resistivity [n=3]
- Fig. 2-2-21 (4) TDIP Plane Map of Apparent Resistivity [n=4]
- Fig. 2-2-21 (5) TDIP Plane Map of Apparent Resistivity [n=5]
- Fig. 2-2-22 TDIP Pseudo-section of Chargeability [Line B-F]
- Fig. 2-2-23 (1) TDIP Plane Map of Chargeability [n=1]
- Fig. 2-2-23 (2) TDIP Plane Map of Chargeability [n=2]
- Fig. 2-2-23 (3) TDIP Plane Map of Chargeability [n=3]
- Fig. 2-2-23 (4) TDIP Plane Map of Chargeability [n=4]
- Fig. 2-2-23 (5) TDIP Plane Map of Chargeability [n=5]
- Fig. 2-2-24 (1) TDIP 2-d. Model Simulation Analysis [Line B]
- Fig. 2-2-24 (2) TDIP 2-d. Model Simulation Analysis [Line C]
- Fig. 2-2-24 (3) TDIP 2-d. Model Simulation Analysis [Line E]
- Fig. 2-2-25 TDIP Interpretation Map
- Fig. 2-2-26 Location Map of Rock Samples
- Fig. 2-2-27 Distribution for Resistivity and Chargeability of Rock Samples
- Fig. 2-2-28 Geophysical Interpretation Map
- Fig. 2-2-29 Location Map of Drill Holes in the Nakoroutari Area
- Fig. 2-2-30 Geologic Log of MJFV-1
- Fig. 2-2-31 Geologic Log of MJFV-2

- Fig. 2-2-32 Geologic Log of MJFV-3
- Fig. 2-2-33 Geologic Profile of MJFV-1
- Fig. 2-2-34 Schematic Alteration Zoning of MJFV-1
- Fig. 2-2-35 Geologic Profile of MJFV-2
- Fig. 2-2-36 Schematic Alteration Zoning of MJFV-2
- Fig. 2-2-37 Geologic Profile of MJFV-3
- Fig. 2-2-38 Schematic Alteration Zoning of MJFV-3
- Fig. 2-2-39 Histograms of Homogenization Temperature from the Nakoroutari Area
- Fig. 2-2-40 Resistivity and Chargeability of Drill Core Samples
- Fig. 2-2-41 Schematic Block Diagram of Drill Holes in the Leli's Prospect
- Fig. 2-2-42 Schematic Block Diagram Showing the CSAMT Simulation Results
- Fig. 2-2-43 Schematic Block Diagram Showing the TDIP Simulation Results
- Fig. 2-3-1 Schematic Stratigraphic Columns of the Dakuniba Area
- Fig. 2-3-2 Sample Location Map of the Dakuniba Area
- Fig. 2-3-3 Summary Map of Existing Data of the Dakuniba Area
- Fig. 2-3-4 Distribution Map of Prospects and Alteration Zones in the Dakuniba Area
- Fig. 2-3-5 Detailed Survey Results of the Dakuniba Prospect
- Fig. 2-3-6 Geochemical Survey Results of the Dakuniba Area
- Fig. 2-3-7 Geochemical Survey Results of the Dakuniba Trenches Area
- Fig. 2-3-8 Histogram of Assay Values(the Dakuniba Area)
- Fig. 2-3-9 Cumulative Frequency Distribution of Assay Values (the Dakuniba Area)
- Fig. 2-3-10 Correlation between Elements (the Dakuniba Area)
- Fig. 2-3-11 Location Map of Drill Holes in the Dakuniba Area
- Fig. 2-3-12 Geologic Log of MJFV-4
- Fig. 2-3-13 Geologic Log of MJFV-5
- Fig. 2-3-14 Geologic Log of MJFV-6
- Fig. 2-3-15 Geologic Log of MJFV-7
- Fig. 2-3-16 Geologic Log of MJFV-8
- Fig. 2-3-17 Geologic Log of MJFV-9
- Fig. 2-3-18 Geologic Profile of MJFV-4
- Fig. 2-3-19 Schematic Alteration Zoning of MJFV-4
- Fig. 2-3-20 Geologic Profile of MJFV-5
- Fig. 2-3-21 Schematic Alteration Zoning of MJFV-5
- Fig. 2-3-22 Geologic Profile of MJFV-6
- Fig. 2-3-23 Schematic Alteration Zoning of MJFV-6
- Fig. 2-3-24 Geologic Profile of MJFV-7

- Fig. 2-3-25 Schematic Alteration Zoning of MJFV-7
- Fig. 2-3-26 Geologic Profile of MJFV-8
- Fig. 2-3-27 Schematic Alteration Zoning of MJFV-8
- Fig. 2-3-28 Geologic Profile of MJFV-9
- Fig. 2-3-29 Schematic Alteration Zoning of MJFV-9
- Fig. 2-3-30(1) Histograms of Homogenization Temperatures of Fluid Inclusions from the Dakuniba Area(1)
- Fig. 2-3-30(2) Histograms of Homogenization Temperatures of Fluid Inclusions from the Dakuniba Area(2)
- Fig. 2-3-30(3) Histograms of Homogenization Temperatures of Fluid Inclusions from the Dakuniba Area(3)
- Fig. 2-3-31 Integrated Profiles of Assay Values and Homogenization Temperatures
-
- Fig. 2-4-1 Schematic Stratigraphic Columns of the Waimotu Area
- Fig. 2-4-2 Sample Location Map of the Waimotu Area
- Fig. 2-4-3 Summary Map of Existing Data of the Waimotu Lodes and Bill's Hill Prospect
- Fig. 2-4-4 Summary Map of Existing Data of the Nuku Prospect Area
- Fig. 2-4-5 Distribution Map of Prospects and Alteration Zones in the Waimotu Area
- Fig. 2-4-6 Detailed Survey Results of the Waimotu Lodes and Bill's Hill Prospect
- Fig. 2-4-7 Detailed Survey Results of the Nuku Prospect Area
- Fig. 2-4-8 Geochemical Survey Results of the Waimotu Area
- Fig. 2-4-9 Geochemical Survey Results of the Waimotu Lodes and Bill's Hill Prospect
- Fig. 2-4-10 Geochemical Survey Results of the Nuku Prospect Area
- Fig. 2-4-11 Histogram of Assay Values(the Waimotu Area)
- Fig. 2-4-12 Cumulative Frequency Distribution of Assay Values (the Waimotu Area)
- Fig. 2-4-13 Correlation between Elements (the Waimotu Area)

TABLES

- Table 1-1 Amount of Work
- Table 1-2 Duration of Survey and Participants
- Table 1-3 Temperature and Precipitation at Savusavu and Labasa
- Table 1-4 Simplified Volcanic Stratigraphy of Vanua Levu
- Table 2-1-1 Major Volcanic Trends in Vanua Levu
- Table 2-1-2 Known Prospects in Vanua Levu
- Table 2-2-1 Equipment of Array CSAMT Method
- Table 2-2-2 Equipment of Time Domain IP Method

Table 2-2-3 Results of Physical Property of Rock Samples

Table 2-2-4 Location, Orientation and Length of Drill Holes in the Nakoroutari Area

Table 2-2-5 Location, Orientation and Length of Drill Holes in the Dakuniba Area

Appendix

Table A-1(1) Results of Microscopic Observation of Thin Sections(1)

Table A-1(2) Results of Microscopic Observation of Thin Sections(2)

Table A-1(3) Results of Microscopic Observation of Thin Sections(3)

Table A-2(1) Results of Microscopic Observation of Polished Thin Sections(1)

Table A-2(2) Results of Microscopic Observation of Polished Thin Sections(2)

Table A-2(3) Results of Microscopic Observation of Polished Thin Sections(3)

Table A-3(1) Results of X-ray Diffraction Analysis of Rock Samples(1)

Table A-3(2) Results of X-ray Diffraction Analysis of Rock Samples(2)

Table A-3(3) Results of X-ray Diffraction Analysis of Rock Core Samples(3)

Table A-3(4) Results of X-ray Diffraction Analysis of Drill Core Samples(1)

Table A-3(5) Results of X-ray Diffraction Analysis of Drill Core Samples(2)

Table A-3(6) Results of X-ray Diffraction Analysis of Drill Core Samples(3)

Table A-4(1) Results of Chemical Analysis of Rock Samples(1)

Table A-4(2) Results of Chemical Analysis of Rock Samples(2)

Table A-4(3) Results of Chemical Analysis of Rock Samples(3)

Table A-4(4) Results of Chemical Analysis of Rock Samples(4)

Table A-4(5) Results of Chemical Analysis of Drill Core Samples(5)

Table A-4(6) Results of Chemical Analysis of Drill Core Samples(1)

Table A-4(7) Results of Chemical Analysis of Drill Core Samples(2)

Table A-4(8) Results of Chemical Analysis of Drill Core Samples(3)

Table A-5(1) Homogenization temperatures of Fluid Inclusions(1)

Table A-5(2) Homogenization temperatures of Fluid Inclusions(2)

Table A-6 Resistivity and Chargeability of Drill Core Samples

PART I OVERVIEW

PART I OVERVIEW

Chapter 1 Introduction

1-1 Background and Objectives

In response to the request by the Government of the Republic of Fiji to conduct mineral exploration in Vanua Levu, the Japanese Government dispatched a mission to discuss the details of the project. As a result of the consultation between the Mineral Resources Department (MRD) of the Ministry of Lands, Mineral Resources & Energy, and Metal Mining Agency of Japan, an agreement was reached for cooperative exploration in Vanua Levu. The "Scope of Work" (SW) was signed by the representatives of both governments in August, 1995. The objective of this project is to explore and assess the mineral potential of the survey area through geological survey, geochemical exploration, geophysical exploration and drilling during a three-year period from 1995 to 1998.

The first phase of this project was carried out during Fiscal 1995. The objective of that phase was to clarify the geological environment and thereby understand the occurrence and conditions of ore deposits of Vanua Levu Island. The work carried out included; compilation of available geological information and data concerning the whole island (areal extent 5,500 km²), geological survey of the three areas, Nakoroutari, Waimotu and Dakuniba Areas, and geophysical survey in the Nakoroutari area.

The second phase was carried out during Fiscal 1996. The objective of this phase was the exploration of the promising zones which were extracted by the first phase survey. The second phase comprised drilling of both three localities within the Nakoroutari area and the Dakuniba Area, respectively.

The third phase was carried out during Fiscal 1997. The objective of this phase was the exploration of the mineralization zone which was encountered by the MJFV-5 drill holes during the second phase survey. The third phase comprised drilling of three localities within the Dakuniba Area.

1-2 Survey Methods

(1) Amount of work

The amount of work is shown in Table 1-1.

Table 1-1 Amount of Work

Phase	Survey Method	Area	Amount
First phase (in 1995)	Compilation of Existing Data	Whole Vanua Levu	A Areal extent 5,500km ²
	Geological Survey (including Geochemical Survey)	Nakoroutari Area Dakuniba Area Waimotu Area	Areal Extent 100km ²
			Length of traverse 200km
Geophysical Survey	Nakoroutari Area	Laboratory work	
		Thin section microscopy 31pcs	
Second phase (in 1996)	Drilling	Nakoroutari Area	Polished section 31pcs
			X-ray diffraction analysis 108pcs
			Chemical analysis 507pcs
Drilling	Dakuniba Area	Array CSAMT	
		Survey length 12km	
Third phase (in 1997)	Drilling	Dakuniba Area	TDIP
			Survey length 7.5km
			Laboratory work
Drilling	Nakoroutari Area	Measurement of Resistivity 30pcs	
		Measurement of Chargeability 30pcs	
Drilling	Dakuniba Area	Number of drill holes 3	
		Total length drilled 901.30 m	
Drilling	Dakuniba Area	Laboratory work	
		Thin section microscopy 30pcs	
Drilling	Dakuniba Area	Polished section 20pcs	
		Homogenization temperature of	
Drilling	Dakuniba Area	Fluid inclusions 12pcs	
		X-ray diffraction analysis 72pcs	
Drilling	Dakuniba Area	Chemical analysis 83pcs	
		Measurement of Resistivity 35pcs	
Drilling	Dakuniba Area	Measurement of Chargeability 35pcs	
		Number of drill holes 3	
Drilling	Dakuniba Area	Total length drilled 901.70 m	
		Laboratory work	
Drilling	Dakuniba Area	Thin section microscopy 15pcs	
		Polished section 12pcs	
Drilling	Dakuniba Area	Homogenization temperature of	
		Fluid inclusions 9pcs	
Drilling	Dakuniba Area	X-ray diffraction analysis 32pcs	
		Chemical analysis 52pcs	
Drilling	Dakuniba Area	Number of drill holes 3	
		Total length drilled 1,101.30 m	
Drilling	Dakuniba Area	Laboratory work	
		Thin section microscopy 10pcs	
Drilling	Dakuniba Area	Polished section 10pcs	
		Homogenization temperature of	
Drilling	Dakuniba Area	Fluid inclusions 5pcs	
		X-ray diffraction analysis 32pcs	
Drilling	Dakuniba Area	Chemical analysis 55pcs	

1-3 Duration of Survey and Participants

The Duration of Survey and Participants is shown in Table 1-2.

Table 1-2 Duration of Survey and Participants

Phase	Contents	Duration	Members	
First Phase (in 1995)	Project finding and Scope of Work consultation	July 30 -August 2	Masaaki NOGUCHI ⁽¹⁾ Masahiro KINE ⁽²⁾ Tsuneyuki UTAMARU ⁽¹⁾ Yuichi SASAKI ⁽⁴⁾ Shigeki SAKURAI ⁽⁴⁾	Bhuwan DUTT ⁽⁴⁾ Abdul RAHMAN ⁽⁵⁾ Vijendra PRASAD ⁽⁵⁾ Devika REDDY ⁽⁵⁾
	Field supervisor	September 25 -September 27	Katsuhisa OHNO ⁽¹⁾	
	Compilation of existing data	September 28 -October 11	Osamu MIYAISHI ⁽⁶⁾ Ken OBARA ⁽⁶⁾ Kenji SATO ⁽⁶⁾ Kazuyasu SUGAWARA ⁽⁶⁾ Masao SUGAWARA ⁽⁶⁾	Devika REDDY ⁽⁵⁾ Subashini DEO ⁽⁵⁾ Isireli NAGATA ⁽⁵⁾ Mohammed FEROUZ ⁽⁵⁾ Moape NAVIA ⁽⁵⁾
	Geological Survey	October 12 -December 21	Osamu MIYAISHI ⁽⁶⁾ Ken OBARA ⁽⁶⁾ KENJI SATO ⁽⁶⁾ Kazuyasu SUGAWARA ⁽⁶⁾	
	Geophysical Survey	October 29 -December 17	Masao YOSHIZAWA ⁽⁶⁾ Toshiaki FUJIMOTO ⁽⁶⁾ Tadanori IWASAKI ⁽⁶⁾	
Second Phase (in 1996)	Drilling	July 1 -November 18	Osamu MIYAISHI ⁽⁶⁾ Hiroshi ISHIKAWA ⁽⁶⁾	Vijendra PRASAD ⁽⁵⁾ Isireli NAGATA ⁽⁵⁾ Moape NAVIA ⁽⁵⁾ Jonati RAILALA ⁽⁵⁾
Third Phase (in 1997)	Field Supervisor	September 13 -September 18	Yuji TOKUMASU ⁽¹⁾	Vijendra PRASAD ⁽⁵⁾ Isireli NAGATA ⁽⁵⁾
	Drilling	June 23 -September 25*	Osamu MIYAISHI ⁽⁶⁾ Hiroshi ISHIKAWA ⁽⁶⁾	

*: September 21 for Hiroshi ISHIKAWA

⁽¹⁾: Metal Mining Agency, ⁽²⁾: Ministry of International Trade and Industry

⁽³⁾: Japan International Agency, ⁽⁴⁾: Ministry of Lands, Mineral Resources and Energy

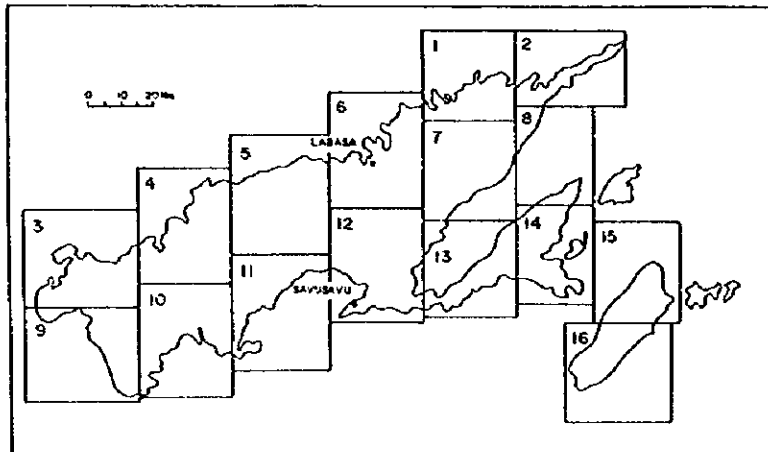
⁽⁵⁾: Mineral Resources Department, ⁽⁶⁾: Nikko Exploration & Development Co., Ltd.

Chapter 2 Outline of Past Geological Surveys

An outline of the geology of Fiji was reviewed and summarized by Rodda (1989), Okuda (1989) and others. Geological maps of Vanua Levu at 1:50 000 have been published covering the whole island by the Geological Survey of Fiji (now the MRD). The sheet number, area and the index map are shown below.

Author, published year and title of the publication	Sheet No.
Bartholomew, R.B. (1959): Geology of Savusavu Bay West, Vanua Levu	11
Rickard, M.J. (1970): Geology of north-eastern Vanua Levu	1,2
Ibbotson, P. (1969): The Geology of east-central Vanua Levu	6,7,8
Coulson, F.I.E. (1971): The Geology of Western Vanua Levu	3,9
Hindle, W.H. (1976): The Geology of west-central Vanua Levu	4,5,10
Woodrow, P.J. (1976): The Geology of south-eastern Vanua Levu	12,13,14

A reconnaissance map at 1:250 000 has been compiled by Rickard (1966). The gold mineralization of the western Pacific region including Fiji has been summarized by Ishihara and Urabe (1989). The metallic mineral deposits of Fiji were reviewed by Colley (1976, 1980) and Colley and Flint (1995) of the MRD. Reports concerning most individual prospects are available at the library of the MRD.



Chapter 3 Geography of the Project Area

3-1 Location and Access

The island of Vanua Levu is approximately 180km east-west, 35km north-south and approximately 5,500 km² in areal extent. It is located at latitude 16°07'S-17°01'S and longitude 178°29'E-179°57'W, and is approximately 2,800 km east of the eastern coast of Australia, approximately 2,000 km north of New Zealand and approximately 2,000km south of the equator.

The major population centers are developed along the coast, namely Labasa, Savusavu and Nabouwalu. Entrance to Fiji is via air and usually through the international airport at Nadi on Viti Levu. Flight from Viti Levu to Vanua Levu by commercial airplane takes 25 minutes via either Nadi or Nausori near Suva. Existing roads circle the island except for the northeastern part. The majority of the main roads between Labasa and Savusavu, and Labasa and Nabouwalu is paved.

3-2 Topography

The island shows generally gentle undulation in the northern part and steep mountainous topographic feature in the southern part. Dominant rivers such as the Dreketi and Labasa Rivers are developed in the northern part of the island and carry silt to the sea, resulting in the development of lowlands with mangrove plants in some areas. The mountains are around 600 m to 900 m in elevation, with the highest peak Mountain Nasorolevu, reaching 1,032 m. The top of the mountain range is gentle in topography, characterized by flat peaks around which a narrow drainage system has developed with numerous waterfalls. The cone shaped volcanoes vary in size such as large Bua Volcano, and in contrast, the smaller one east of the Viani Bay.

3-3 Climate and Vegetation

As Vanua Levu belongs to the tropical rain forest climatic zone, it has two seasons, dry (April-November) and wet (December-March). Also, it is located in the monsoon zone and there is a southeasterly trade wind throughout the year. Precipitation on the northern side of the island is relatively low, and high on the southern side. The monthly temperatures and precipitation observed at Labasa and Nabouwalu are listed below.

Table 1-3 Temperature and Precipitation at Savusavu and Labasa

(Data in 1996)

Location		Jan	Feb	Mar	Apr	May	June	July	Aug	Sept	Oct	Nov	Dec	Annual	
Savusavu	Temperature (°C)	high	30.5	30.3	-	30.6	28.5	27.6	28.1	27.0	28.0	28.0	29.5	30.5	29.0
		low	24.1	24.4	-	23.7	22.3	22.4	21.7	21.7	22.6	22.3	22.3	22.7	22.7
	Precipitation (mm)	352	147	193	135	272	327	81	26	76	378	159	265	2,415	
Labasa	Temperature (°C)	high	31.2	32.2	31.8	32.1	29.7	29.2	29.9	29.5	30.1	30.2	31.5	32.3	30.8
		low	22.9	22.0	22.7	21.5	20.1	20.0	18.1	18.3	20.1	20.4	21.5	-	20.7
	Precipitation (mm)	532	-	453	93	209	264	76	11	123	119	92	290	2,262	

Chapter 4 General Geology of the Survey Area

4-1 Geologic Setting: Plate Tectonics

Tectonically, the Fijian islands are located at the eastern margin of the Indo-Australian Plate and form an island arc on an ocean ridge (Lau Ridge) at a point where it bends from the ENE-WSW to N-S direction. At the Tonga trench on the eastern side of the Tonga Arc, which is located to the east of the Lau Ridge, the Pacific Plate is being subducted westward at the Vanuatu Trench on the western side of the Vanuatu Arc located to the west of the Fijian islands.

The Lau basin is located between the Tonga Arc and the Lau Ridge, and the North Fiji Basin between Vanuatu and Viti Levu. Both these basins have spreading axis. The northern side of Vanua Levu is bounded by the left lateral Fiji Transform Fault, and the southern side by the Hunter Fracture Zone, a left lateral transform fault. The northern part of the Fijian Islands is considered to be rotating anticlockwise due to the eastward movement of the Indo-Australian Plate south of the Hunter Fracture Zone and the spreading of the North Fiji Basin. This rotation is believed to have begun during Miocene and Early Pliocene time. Before the advent of the spreading of the North Fiji Basin, Eocene - Miocene chain of island arcs (Vanuatu Arc - Fiji Islands - Tonga - Lau Arc), continuous in the NW-SE to N-S direction, are believed to have existed due to the subduction of the Pacific Plate at the Tonga Trench and its northward extension.

The geology of the Fijian Islands consists totally of Cenozoic units. The oldest unit is Eocene (limestone and volcanic rocks) in age while the youngest is represented by the volcanic ejecta of historic times originating Taveuni Island. In Vanua Levu, the geologic units are characterized by Late Miocene to Late Pliocene strata and consists mainly of volcanic rocks (basalt, andesite, dacite) accompanied by sandstone, mudstone and marl. At the Udu Peninsula in the northeast, felsic volcanic rocks are dominant. Taveuni Island is underlain by

Pliocene and later basalts with volcanic activity continuing to recent times. The islands on the Koro Sea consist of Pliocene to Pleistocene basalts. The Lau Islands are underlain by Middle Miocene to Quaternary strata that are mainly composed of volcanics (basalt, andesite, dacite, and rhyolite) and accompanied by limestones. Kadavu Islands consist of Middle Pliocene to Pleistocene volcanic rocks. The Mamanuca and Yasawa Islands are underlain by volcanic rocks with intercalated pelagic limestone.

4-2 Geologic Setting of the Survey Area

Stratigraphically, Vanua Levu is underlain in most areas by Late Miocene to Pliocene strata that consist of basalt, andesite and dacite with intercalated sandstone, mudstone, and marl. The volcanic rocks are classified largely into the Natewa Volcanic Group, the Monkey Face Volcanic Group, the Udu Volcanic Group, the Nararo Volcanic Group and the Bua Volcanic Group.

Table 1-4 Simplified Volcanic Stratigraphy of Vanua Levu

Geologic Unit Name	Main Lithology	Thickness	K-Ar Age
Bua Volcanic Group	Basalt	more than 900 m	(3.3-2.8 Ma)
(Uluikamali Formation)	Basalt-andesite	at most 200 m	(4.7-4.4 Ma)
Nararo Volcanic Group	Acidic andesite		
Udu Volcanic Group	Dacite Rhyolite	more than 300 m	(7.0-6.8 Ma)
Monkey Face Volcanic Group Natewa Volcanic Group	Andesite	more than 1500 m	(7.5-3.5 ma)

4-3 Brief History of Mining in the Survey Area

Various types of mineralization are known in Vanua Levu and there are many prospects and some mines. The major types of mineralization are kuroko, epithermal veins, and dissemination. Bauxite ore deposits also occur on the western part of the islands.

(1) Kuroko type deposits

Kuroko type deposits occur on the Udu Peninsula in the northeastern part of Vanua Levu. They are called the Udu deposits (Nukudamu deposits) and discovered in 1957, followed by the drilling of 381 holes during 1957 to 1968. In 1968, Thirty two thousand tons of ore at the average grade of 5.9% Cu and 6.7% Zn was mined before ceasing operations.

The Udu deposits occur in the intensely altered pumice bearing Udu Volcanic Breccia. The deposits are distributed within approximately 450 m x 200 m area. The main ore body has a pipe-like shape covering 300 m

× 120 m in plan and plunges 20-30° to the ESE. The ore occurring the center of the pipe is mainly composed of massive sulfide and has undergone argillization, silicification and pyrite dissemination. Disseminated ore is dominant in the surrounding area. The massive ore displays a zonation composed of black ore, yellow ore and sulfide ore in descending order. The main ore minerals are: pyrite, sphalerite, tennantite and barite, while chalcopyrite is scarce compared to the Japanese equivalents. The Mouta and Wainikoro prospects are also well known.

(2) Epithermal gold deposits

The main epithermal type prospect is at Mount Kasi in the southwestern part of the island. The deposit was mined by the open cut method during 1932 to 1946 with an estimated production of around 60,000 ounces of gold. An estimated 265 thousands tons of ore grading 7g/tAu was treated. The mineralization encompasses an area of 10km²

Gold mineralization occurs in quartz barite veins along faults hosted by calc-alkaline andesite. The main ore deposit strikes NW-SE and dips steeply westward. The mined ore zone extends 300 m in length, 12 m in width, and 30 m vertically. The hanging wall of the fault which hosts the ore is brecciated, with the width of the mineralized zone becoming wider at shallower depths. The brecciated zone is 25 m in maximum width, gold-bearing and silicified. The deposits are classified as epithermal, high sulfidation type. Constituent minerals are native gold, pyrite, chalcopyrite, tetrahedrite and arsenopyrite.

The average grade is in the order of 7 g/tAu and 0.6 g/t Ag. The upper part of the brecciated zone tends to show higher grades, which reach 92 g/tAu. The lower part of the deposit tends to increase in base metal grades with a maximum of 7.2 % Cu, 37 % Zn and 3.6 % Pb. Host rocks have undergone silicification and alteration to alunite and barite in the zone immediately adjacent to the ore deposits, and propylitization including chlorite, calcite, pyrite, sericite and epidote on a regional scale.

(3) Dissemination type mineralization

A wide alteration zone is located around Koroinasolo village. The area is underlain by basaltic-andesitic volcanic rocks and marine sediments of the Miocene-Pliocene Koroma formation. Silicification, opalization and brecciation have developed. The areal extent of propylitic alteration is about 25km². Geochemical anomalies of Au and As in soil are extracted. Disseminated ore deposits of porphyry type are expected.

However, in recent years the area is being explored for epithermal type gold deposits. Mineralization occurs along faults and in shear zones. Especially attractive gold grades have been identified along two major faults that have undergone intense silicification.

Other disseminated type mineralization occurs at the Savudrodoro prospect. The area is underlain by the Savudrodoro Volcanics (basalt lavas and volcanoclastic rocks) and gabbroic dykes. Propylitic alteration and pyrite dissemination occur extensively, especially near the dykes. Geochemical survey and drilling indicate small-scale porphyry copper type mineralization and associated alteration.

Chapter 5 Conclusions and Recommendations

5-1 Conclusions

During the first-phase of the Vanua Levu mineral exploration project; three promising areas (100 km²), namely Nakoroutari, Dakuniba, and Waimotu were delineated by analysis and interpretation of existing geological and mineral resources data and information of the island (5,500 km²). Geological and geochemical surveys were carried out in these three areas and Array CSAMT and time-domain IP survey were made in the Nakoroutari Area. Several promising zones were extracted in these areas. Drilling was conducted in the Nakoroutari Area during the second year and in the Dakuniba Area during the second and third years. The three areas were concluded as follows:

5-1-1 Nakoroutari Area

- (1) This area comprises an areal extent of 36km² and is located approximately 15km south of Labasa. Geochemical, surface magnetic, and IP surveys had been conducted since 1988 in the Leli's Prospect. Also six holes with a total depth of 1,053 m had been drilled in this prospect. The holes were aimed at a quartz breccia zone associated with the NNW-SSE fault system and encountered ores with a core thickness of 0.6 m at 11.6 g/tAu.
- (2) The geology of this area is composed mainly of basalt-andesite lava and volcanics of the Koroutari Andesites, and andesitic volcanics of the Sueni Breccia. These units belong to the Upper Miocene-Lower Pliocene Natewa Volcanics Group.
- (3) Four zones were selected from the study of existing geological and resources data and information. They are; Leli's Prospect, a zone to the south of the same Prospect, Navakuru, and Mugsy's Prospect. Mineralization and alteration were found to occur in all five zones. The Leli's Prospect was concluded to be the most promising by geological survey. It was noted that the altered zone to the south of Leli's Prospect show evidence of gold mineralization.
- (4) The Leli's Prospect occurs within the quartz vein-breccia zone developed in the Koroutari Andesite lava-volcanics which belong to the Natewa Volcanic Group. There are two quartz vein-breccia zones, the eastern and western zones, part of the NNW-SSE system. A silicified tuff breccia sample with a grade of 12.9 g/tAu was collected near the Leli's Prospect, and although in a limited area, high-grade zones had been confirmed during the first year survey.
- (5) Geophysical survey by array CSAMT was carried out for 12km and time domain IP for 7.5km at

the Leli's Prospect.

(6) The array CSAMT method identified intrusive-shaped high resistivity zones in the central parts of Line B-C and Line D-F. One-dimensional resistivity structure analysis showed the existence of two buried high-resistivity bodies that extend in the N-S direction. These two bodies as a whole extend in the NW-SE direction and are interpreted to be areas of silicification.

The apparent resistivity measured by the time domain IP method resulted in a distribution pattern harmonious with the results of the array CSAMT. The chargeability background is dominantly low. Chargeability anomalies exceeding 10 mV-s/V were detected at three localities, but they are independent anomalies and the reliability is very low. Weak anomalies of over 5 mV-s/V occurred continuously in the central-western part of all traverse lines. It was inferred from the results that these IP anomalies were caused by bodies 100 m below the surface. Also the simulation results indicate that these bodies have chargeability in the general range of 5-7 mV-s/V and most probably formed by pyrite mineralization. These bodies and the two high-resistivity bodies detected by the Array CSAMT are located in approximately the same locality. Thus, it was believed that pyritization and silicification were closely related in this area.

(9) Resistivity and chargeability of 30 rock samples (including core samples) were measured in the laboratory. The resistivity of silicified rocks was the highest at 2,884 ohm-m, followed by basalt > andesite > volcanoclastic rocks. The chargeability of volcanoclastic rocks was the highest at 11.7 mV-s/V, followed by silicified rocks > andesite > basalt. It was shown from this work that identification of rock types from physical characteristics was difficult.

(10) Three holes MJFV-1, MJFV-2, and MJFV-3 drilled in the Nakoroutari Area all confirmed two zones of clay quartz veins. In the holes MJFV-2 and -3, weak silicified zones were confirmed in deeper parts. The clay quartz veins confirmed by this drilling strike in the NNW direction and were concluded to continue 600 m in the strike direction. Although the veins encountered in MJFV-1 and -3 are thin, grades of about 5 g/tAu were obtained by assay, and thus the surface gold showings were confirmed to continue into deeper zones. The Au content of the weakly silicified zones, however, was low.

(11) The IP anomalies obtained by CSAMT and IP surveys during the first year were inferred to reflect the deep-seated silicified zones confirmed by MJFV-1 and -3. Thus, it was clarified by the work during second year that the surface mineral showings continue downward to the deeper parts, and that the geophysical anomalous zones correspond to the silicified zones.

(12) Evidences regarding stronger mineralization in the vicinity, however, could not be obtained, and it is believed that the mineral showings confirmed by the first and second year surveys represent the characteristics of the mineralization of this area.

5-1-2 Dakuniba Area

- (1) This area is located approximately 65km east of Savusavu with an areal extent of 36km². A zone comprising WNW-ESE striking quartz veins occurs 1km north of Dakuniba Village in the upper reaches of the Nagagani Creek. The zone was previously explored and is called the Dakuniba Prospect. In the past, two holes with a total length of 176 m had been drilled; soil and rock geochemical survey, CSAMT geophysical survey, and trenching were carried out.
- (2) The geology of this area consists of basaltic lava and volcanics of the Dakuniba Basalt belonging to the Upper Miocene - Lower Pliocene Natewa Volcanic Group.
- (3) Mineralization occurs in the quartz veins developed in the basaltic lava and volcanics. The major veins are developed over 2km in length and strike WNW-ESE and dip steeply. Alteration associated with mineralization is observed in the northeastern part of the area: quartz-clay veins extending from the upper reaches of the Wailevu Creek to the Nagagani Creek, argillized and pyrite dissemination from the Nubuni Creek westward, and mineralization observed in the quartz veins of a tributary of the Waikava Creek.
- (4) The continuity of individual quartz veins exposed in the upper reaches of the Nagagani Creek had not been confirmed. The grade of the quartz veins was high with a maximum of 16 g/tAu and 21 samples containing more than 1 g/tAu were collected from 1km long outcrop. Thus, this zone was concluded to be promising.
- (5) Many quartz veinlets were encountered in MJFV-6. MJFV-5 is at a distance of about 550 m and the correlation between the ores of these two drill holes was difficult. The veins confirmed in MJFV-6, aside from the above were; many quartz veinlets in the shallow (55-96 m) part, and pyrite dissemination-silicification-argillization zone in the deeper part (near 225-300 m). Although these were low grade to barren, they were very interesting.
- (6) As above, gold mineralization, and the associated fissure system and alteration were clarified by the three holes drilled during this year. These agree largely with the strike and dip of the mineral showings on the surface, confirming the continuation of the mineral showings into the deeper subsurface zones. The mineralization confirmed at MJFV-5 was promising and it was necessary to clarify the extension of the veins laterally and vertically toward MJFV-6.
- (7) Further drilling near The MJFV-5, therefore, three drill holes were drilled in the Dakuniba Area during the third year. All three holes, namely MJFV-7, -8, and -9 encountered argillized zone accompanied by silicified breccia. The existence of this zone in these drill holes was inferred from the results of the investigation of surface outcrops and trenches, and drilling at MJFV-4, -5, and -6 carried out during the second year.
- (8) The hole MJFV-7 penetrated argillized zone with quartz breccia-silicified breccia at 226.60-228.00 m depth (1.40 m thick), 249.90-253.70 m depth (3.80 m thick), and 259.10-260.20 m depth (1.10 m thick).

The grade was 0.41g/tAu, 0.47g/tAu, and 0.27g/tAu respectively. Of the above gold-bearing horizons, the grade at 227.50-227.60 m (0.10 m thick) and 251.05-251.20 m depths (0.15 m thick) was 2.3g/tAu and 3.1g/tAu respectively, they are exceeding 1g/tAu.

(9) The hole MJFV-8 confirmed the existence of the mineralized zone at three horizons. The zone encountered at 116.80-129.25 m depth (12.45 m thick) was a clay vein including a silicified zone and the grade was 0.23g/tAu, 0.55g/tAu, 0.64g/tAu, .32g/tAu, 0.63g/tAu, and 1.9g/tAu at depths of 116.80-117.25 m (0.45 m thick), 118.10-118.60 m (0.50 m thick), 122.10-123.80 m (1.70 m thick), 124.30-124.70 m (0.40 m thick), 125.10-127.70 m (2.60 m thick), and 128.15-129.25 m (1.10 m thick) respectively. The altered zone at 141.45-141.70 m (0.25 m thick) and 142.60-143.00 m depths (0.40 m thick) contained 0.47g/tAu and 0.47g/tAu respectively. The gold content of the silicified zone at 279.90-280.70 m depth (0.80 m thick) was less than 0.08g/tAu.

(10) In the hole MJFV-9, there are many quartz-calcite veins between 87.20 m and 93.35 m depths, and gold content of 1.01g/tAu, 0.46g/tAu, and 0.34g/tAu was confirmed at 87.20-87.30 m (0.10 m thick), 88.10-88.45 m (0.35 m thick), and 90.70-94.75 m (4.05 m thick) respectively. The interval of 93.15-93.45 m (0.30 m thick) showed particularly high gold content of 2.3 g/tAu, the highest value of MJFV-9.

(11) The major ore zones encountered by the three MJFV-7, -8 and -9 drill holes; namely the three zones between 226.60-260.20 m depth of MJFV-7, silicified argillized zone at 116.80-119.25 m depth of MJFV-8, and the quartz-calcite veinlet zone at 87.20-95.35 m depth of MJFV-9 were confirmed to be continuous to the quartz breccia-bearing silicified breccia clay zone encountered in MJFV-5 with a WNW-ESE strike. Thus, the continuity of the mineralized zone inferred from the results of the second year survey to exist for 700 m from MJFV-4 to -6 was confirmed in the subsurface part of the area.

(12) Although the assay results of cores obtained from MJFV-7, -8, and -9 are lower than that of MJFV-5, the grade distribution agrees with the general eastward dip. This mineralized zone extends further east and westward, but its surface showings are weak.

(13) The host for the mineralization is basalt and basaltic volcanoclastic rocks. It is fine-grained or vitreous autobrecciated lava and hyaloclastite in the western part, while volcanoclastic rocks are dominant in the eastern part. The fact that the gold grade is higher in the autobrecciated rocks and hyaloclastites in the east indicates the possibility of control of mineralization by the lithology of the host rock.

(14) The formations are gently folded and generally dip gently eastward from MJFV-4 in the west to MJFV-6 in the east. Therefore, the formations encountered in the west are stratigraphically lower than those in the eastern part. Namely, the fine-grained to vitreous autobrecciated lava-hyaloclastite in the west are considered to be at horizon lower than the volcanoclastic rocks in the lower part of the eastern part.

(15) The fluid inclusions of the quartz veins in the east show lower temperature than those from the western part.

(16) X-ray diffraction studies show that the altered minerals are more widely distributed in the east than in the west. Since chlorite occurs widely on the surface in the east, it is more reasonable to infer that the

center of alteration was in the east than to consider this as the indication of shallow parts of the alteration zone in the east.

(17) The distribution of altered minerals clarified by the results of studies regarding; gold grade distribution, fluid inclusion data, and X-ray diffraction data reported above alone is not sufficient for inferring the mineral prospectivity in the lower subsurface zone of the area. Also the mineral potential of other areas is difficult to consider since only surface data are available. However, since widespread gold mineralization was confirmed in the Nagagani Creek area, it is believed that Nagagani and other parts of the present area have sufficient mineral potential for further exploration.

5-1-3 Waimotu Area

(1) The Bill's Hill Prospect is located approximately 45km northeast of Savusavu, and the Waimotu Lode and Nuku Prospect are 0.5km and 2.5km east-northeast from there.

(2) A total of 18 holes had been drilled in the three prospects of this area. A total of 551 m adits was dug and seven holes with a total of 609 m length were drilled into the Waimotu Lodes, seven and four holes were drilled in the Bill's Hill Prospect and Nuku Prospect, respectively.

(3) The geology of this area consists mainly of weakly propylitized andesite and basaltic lava and volcaniclastics of the Koroutari Andesite and Korotini Breccias. These units belong to the Natewa Volcanic Group.

(4) The Waimotu Lodes are comprised of Main Lode, East Lode, and West Lode. A length of about 70 m was confirmed for the Main Lode in outcrop, but both mineralization of the East and West Lodes were confirmed only at one outcrop and the entrance of the adit. All three veins had N-S strike and with a dip of 75° - 90° east for the Main and East Lodes. The widths of the veins were, 1.2 m maximum for the Main Lode and 0.8 m was confirmed at an outcrop for the East Lode. The maximum grade was 24.2 g/tAu for the Main and 42.5 g/tAu for the East Lodes. The gold content of 42.5 g/t was obtained in a sample collected from the East Lode (0.8 m wide), but a sample collected only 1 m south of this sample contained only 2.4 g/tAu, thus the fluctuation in the grade was strong. On the other hand, the average grade of four samples collected along the 70 m length of the Main Lode was 7.2 g/tAu and the gold content is constant. The grade of the West Lode was the lowest of the three at 0.92 g/tAu.

(5) Silicified and argillized zones are well developed in the Bill's Hill Prospect. Quartz and chalcedony stockwork is developed cutting through these zones, and its strike is N-S and the eastward dip is generally steep. Surface observation of the stockwork showed the occurrence of geothite as an opaque with very minor amount of chalcopyrite. The cores drilled in the past showed strong dissemination of pyrite in the silicified zone. The maximum grade of individual veinlets of the stockwork was 0.21 g/tAu.

(6) At Nuku, a silicified zone comprising chalcedony-quartz veins extends in a N-S direction for approximately 150 m and the average width of this zone was approximately 7 m.

(7) The direction of dip was seemingly east, but it was difficult to determine the dip on the surface and from the results of the past drilling, it was inferred to be westward dipping. The highest grade of the stockwork was 4.3 g/tAu (sampled width 2.5 m) and the average of the total 150 m was 1.3 g/tAu (average sampled width 7 m). The past two holes encountered ores at approximately 50 m below the surface and the average grade over a 7 m width was 0.6 g/tAu.

(8) The lower parts of the three prospects in this area had been drilled. All three had significant mineral potential and the zone extending from the lower part of the Waimotu Lode to the subsurface part of eastern Bill's Hill was concluded to be an interesting target for further exploration.

5-2 Recommendations

5-2-1 Nakoroutari area

(1) The geology, alteration, and the characteristics of the gold mineralization of this area were clarified by the work carried out during the first and second years of this project. Drilling in this area (MJFV-1, -2, -3) confirmed the ores in both drill holes would be 600 m apart in the strike direction (NNW-SSE). Judging from the widths and gold grades of the veins that drill holes encountered, however, it is not felt that promising gold deposits are emplaced in this area. No further work in this area is recommended.

(2) On the other hand, the Nakoroutari area is located within the Labasa caldera near its inner slope. Within the caldera hot springs and mineralization zones occur although the volcanic center has not identified because extensive erosion has destroyed the topography. Therefore, it may be effective to evaluate the potential of the area and Leli's Prospect since it may be not the center of mineralization and a more attractive area may be outlined.

5-2-2 Dakuniba Area

The work carried out during the three years of this project was successful in locating gold mineralization in the upper reaches of the Nagagani Creek. It is believed that, however, without additional data, it will not be efficient to immediately attempt to verify high-grade ore zone sufficiently large for development only in this area.

It has been shown by surface geochemical surveys and sampling that there are areas other than the upper Nagagani Creek where, although of low analytical values, gold anomalies cover large areal extent. Only the upper Nagagani area has been surveyed by CSAMT where gold mineralization was confirmed by drilling. And it is most desirable to apply regional survey methods including geophysics to these other anomalous areas, delineate target areas for drilling, and then on the basis of this work, decide on the most

prospective areas for detailed investigation.

Thus, it is recommended that targets other than upper Nagagani be delineated by regional exploration for future exploratory work.

5-2-3 Waimotu Area

Following the first phase survey results, further work in the Waimotu area is recommended. The Waimotu Lode and Bill Hill Prospect are most interesting within the area.

Therefore, it is recommended that we first confirm the downward continuity and the distribution of the new veins parallel to the known three veins, by electric survey, namely CSAMT and IP, then follow it up by drilling.

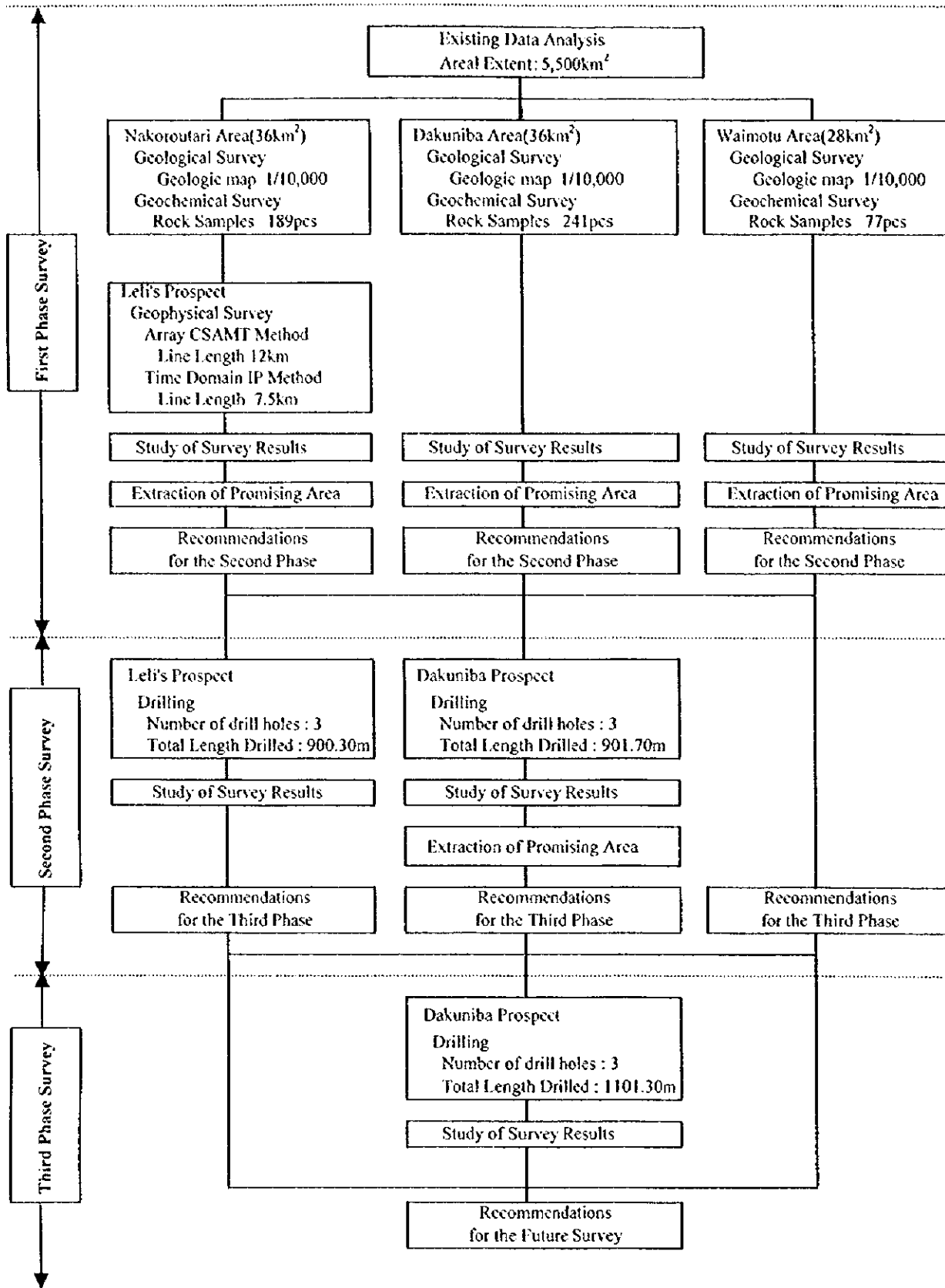


Fig. 1-2 Flow-sheet of the Survey

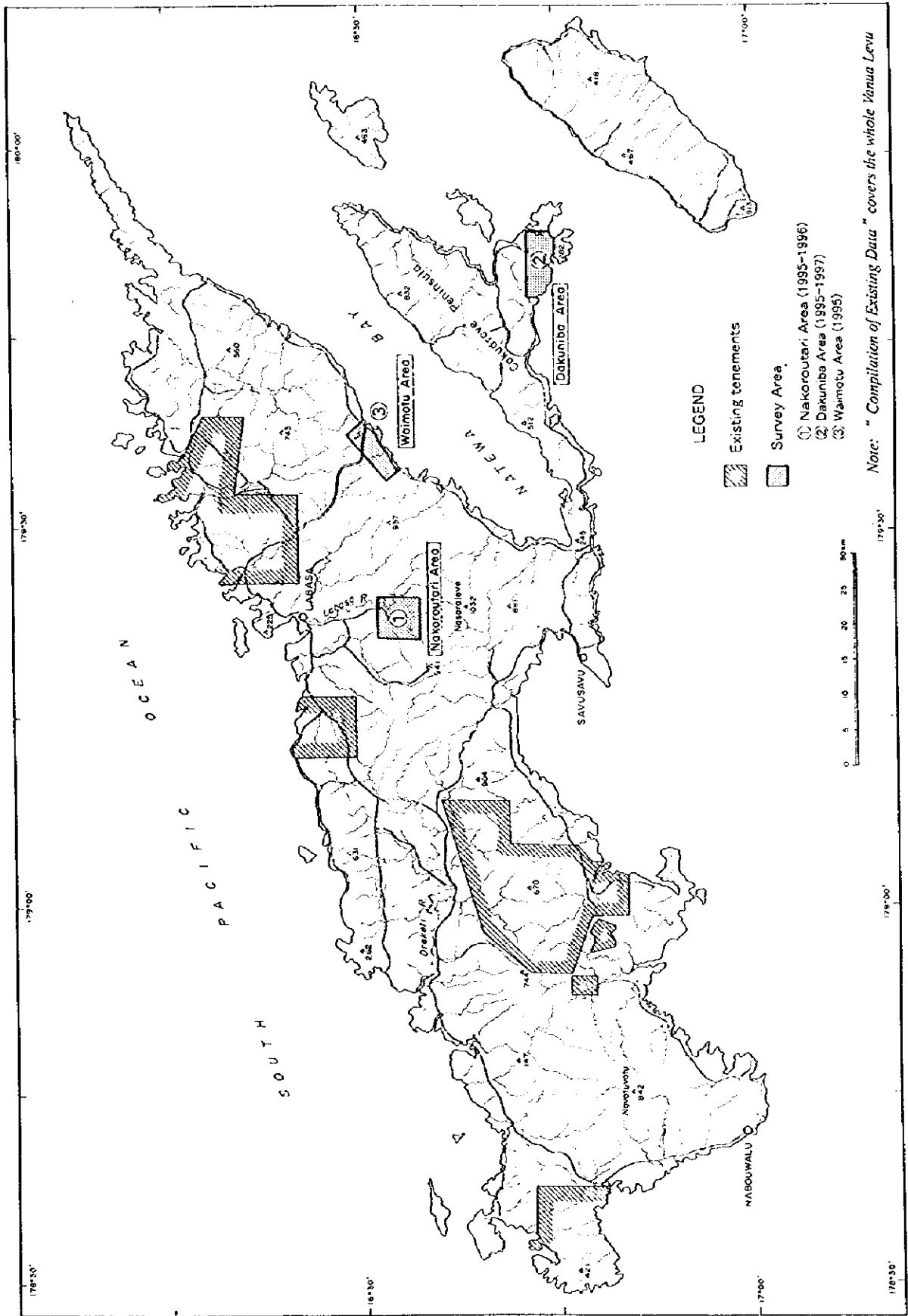


Fig. 1-3 Location Map of the Survey Area

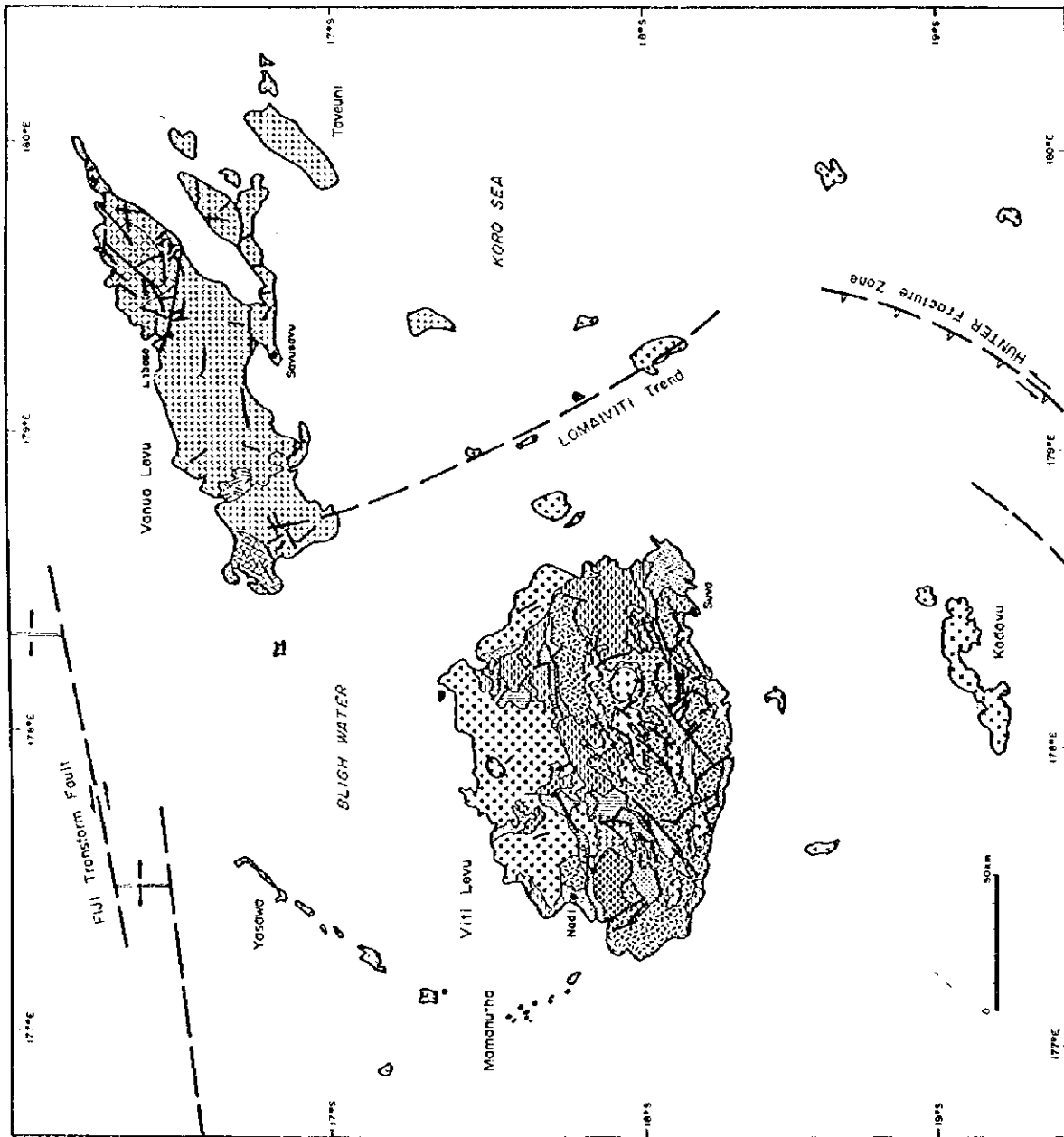


Fig. 1-4 Simplified Geologic Map around the Survey Area

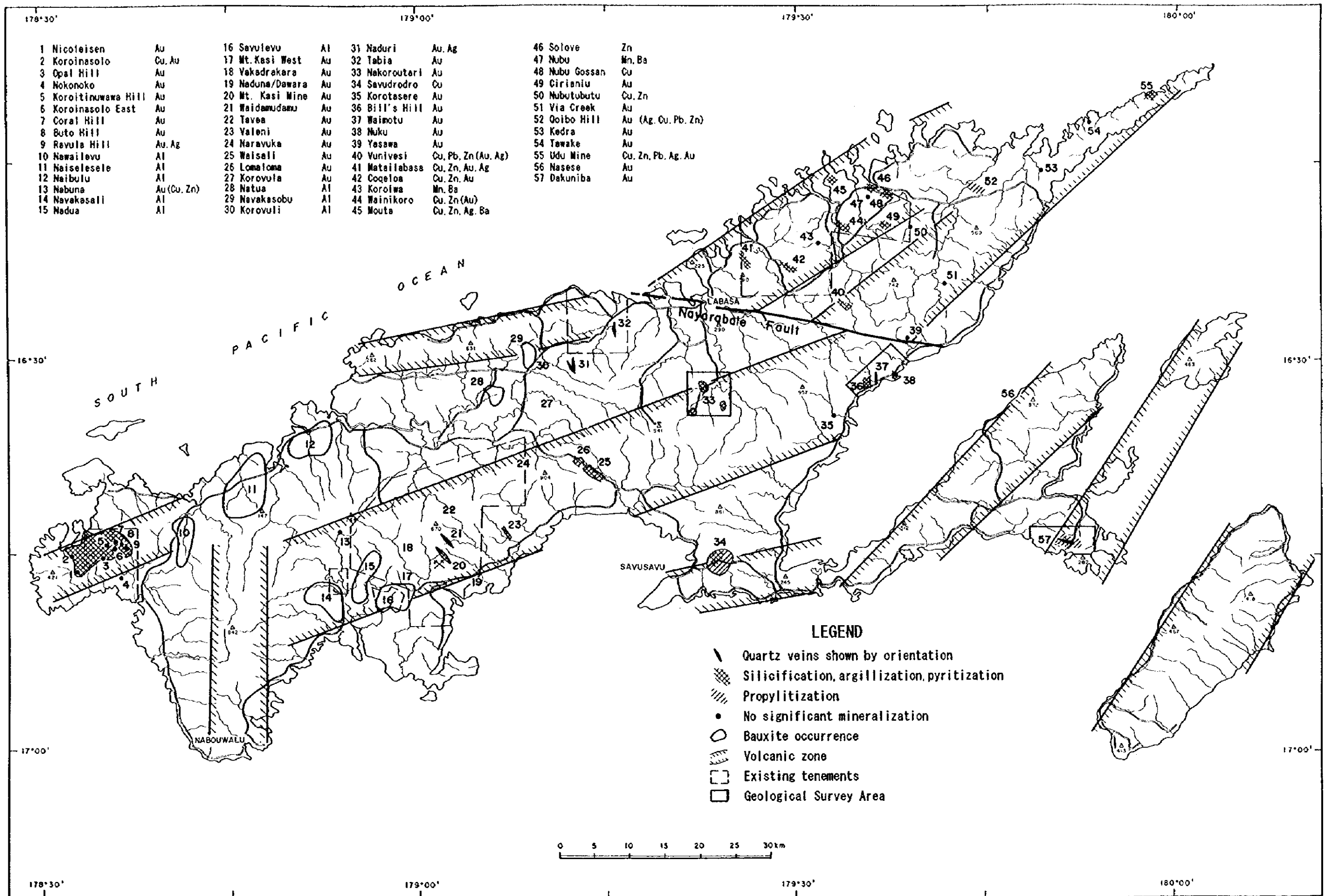


Fig. 1-5 Integrated Interpretation Map of Data Compilation Area

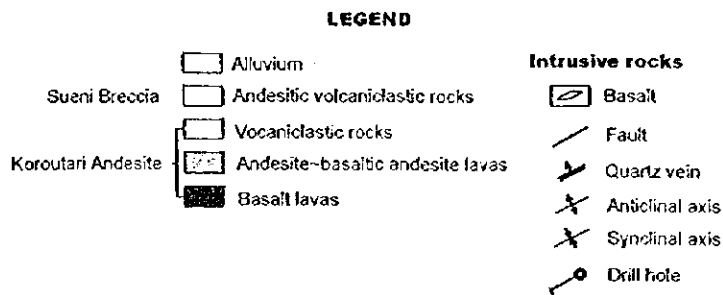
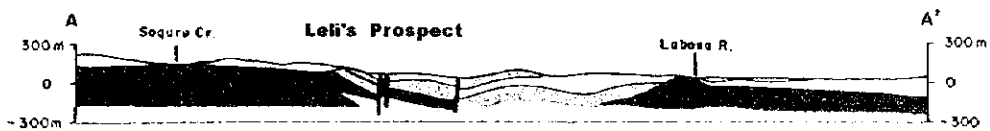
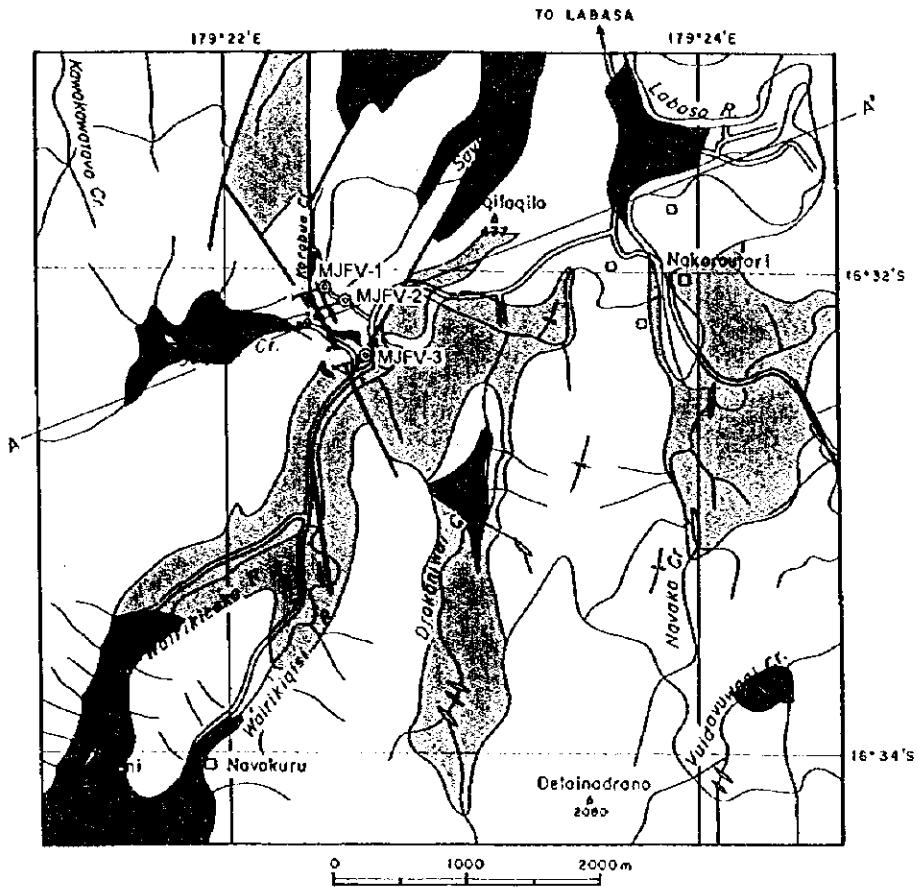


Fig. 1-6 Integrated Map of the Nakoroutari Area

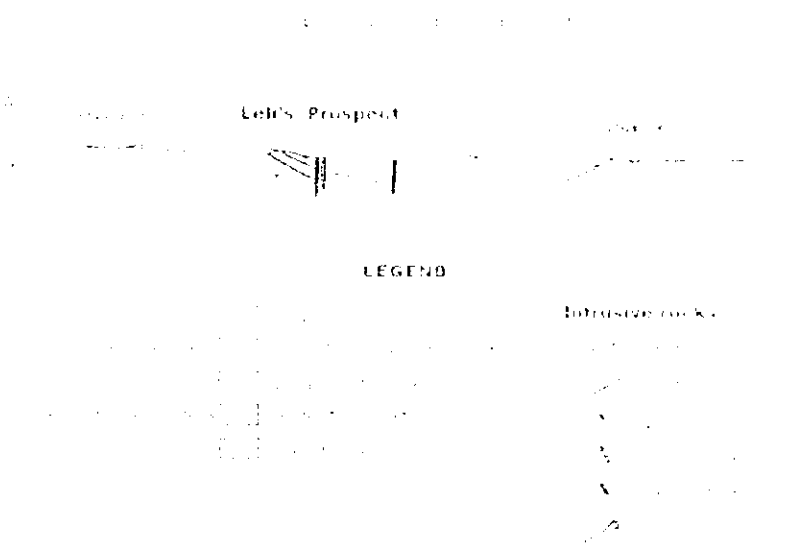
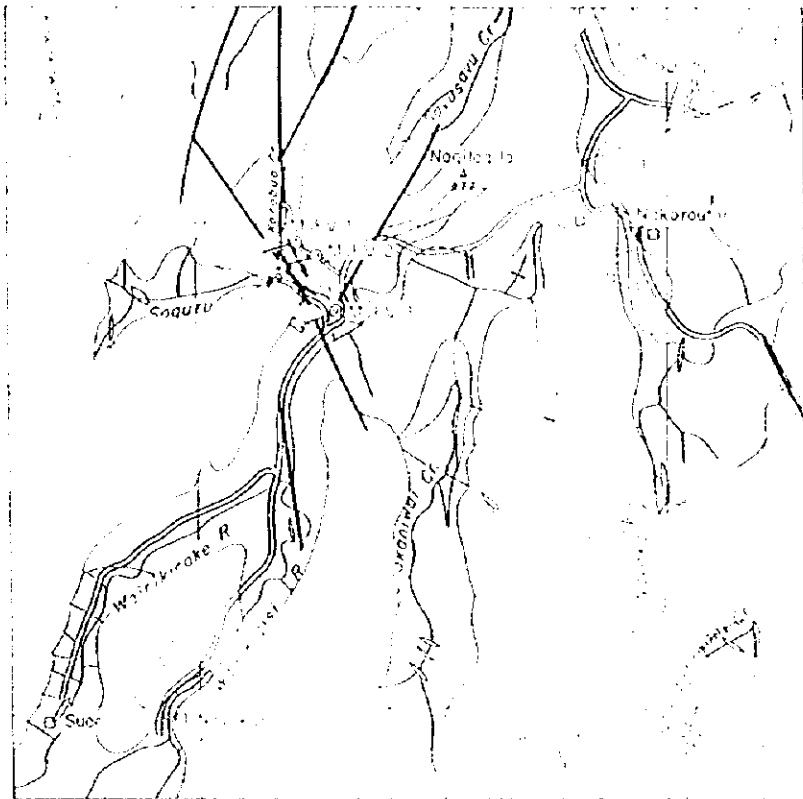


Fig. 16. Geopitani Map of the Nakomatani Area.



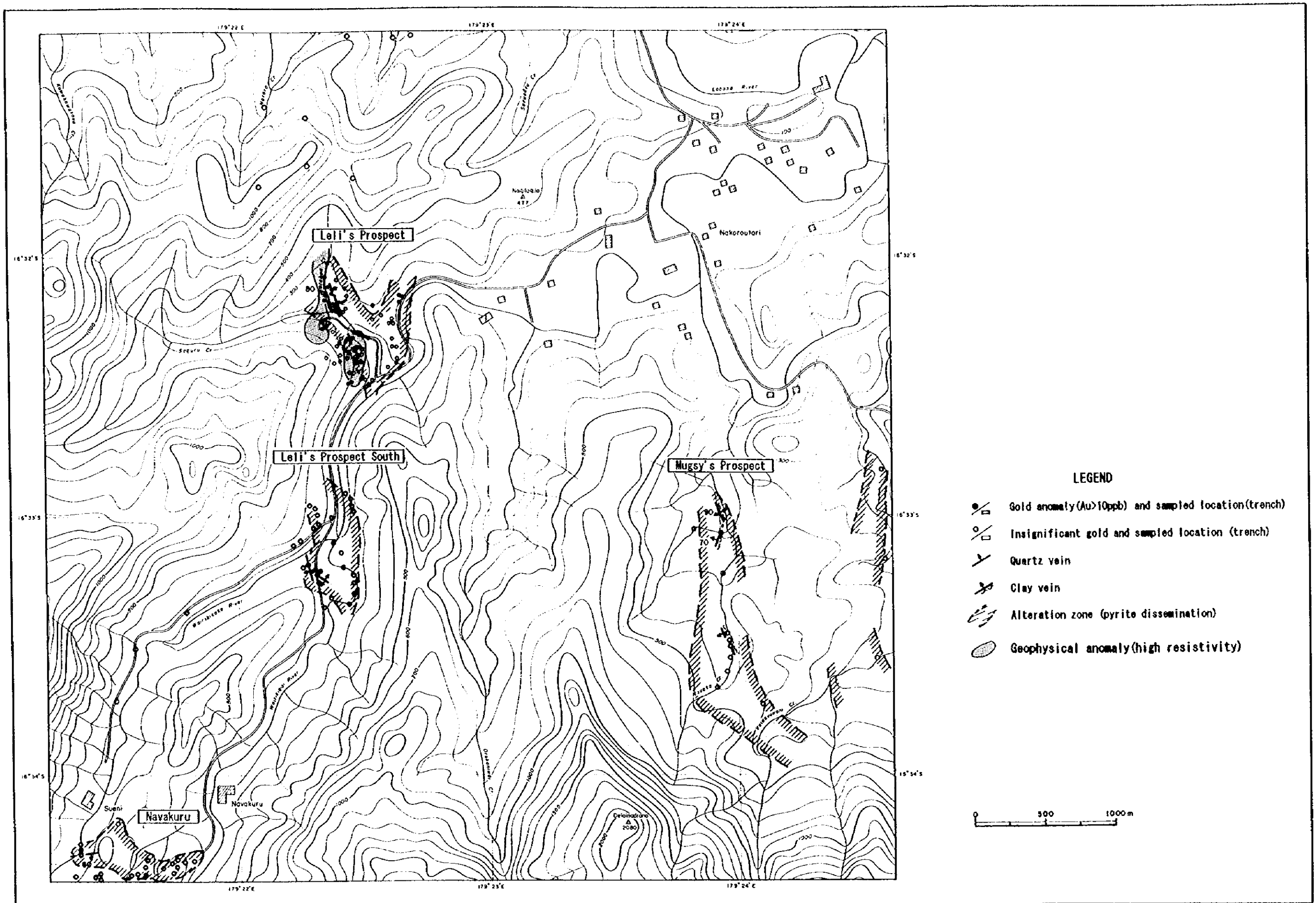


Fig. 1-7 Survey Results of the Nakoroutari Area

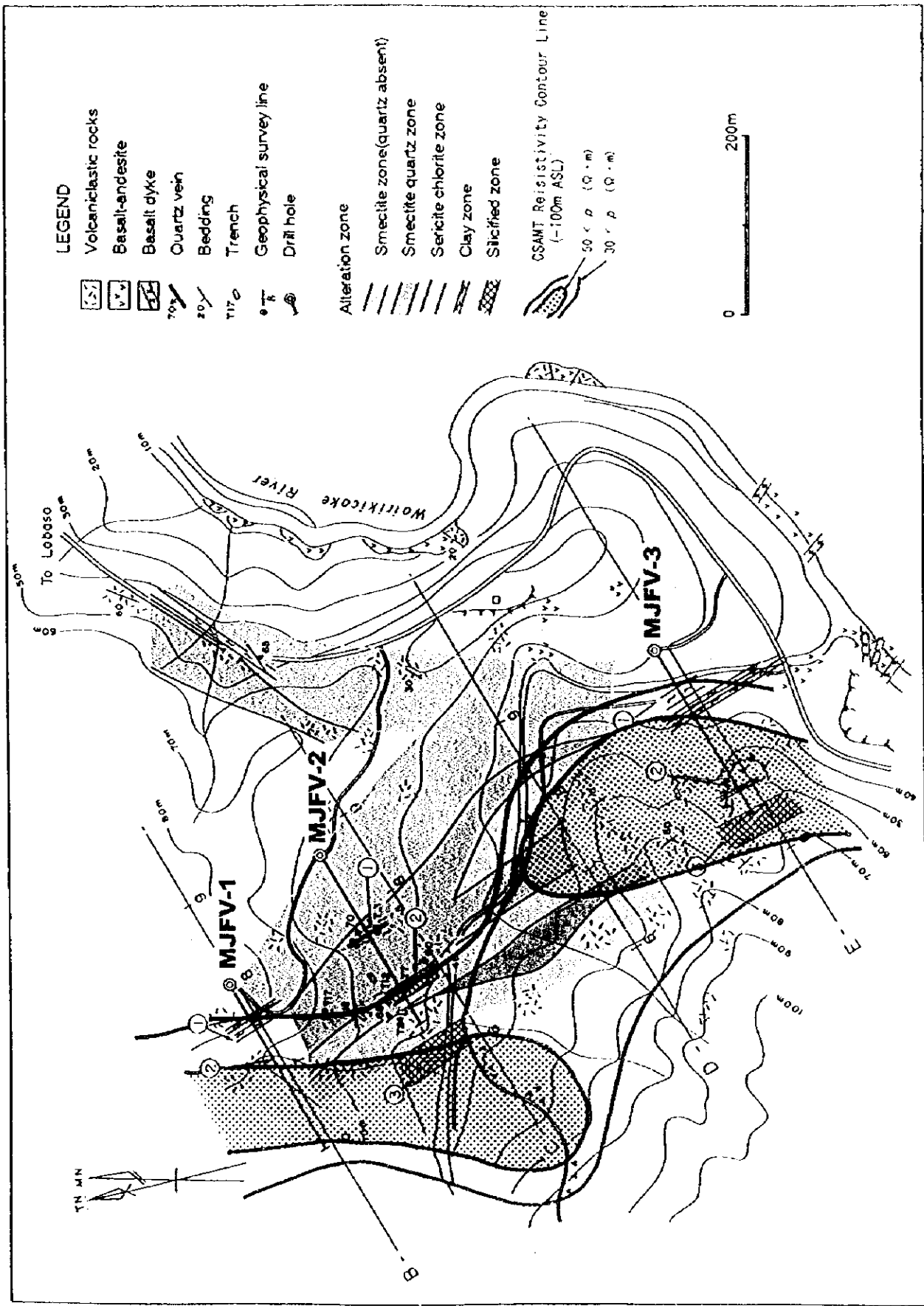


Fig. 1-8 Detailed Survey Results of the Leif's Prospect

10

11

12

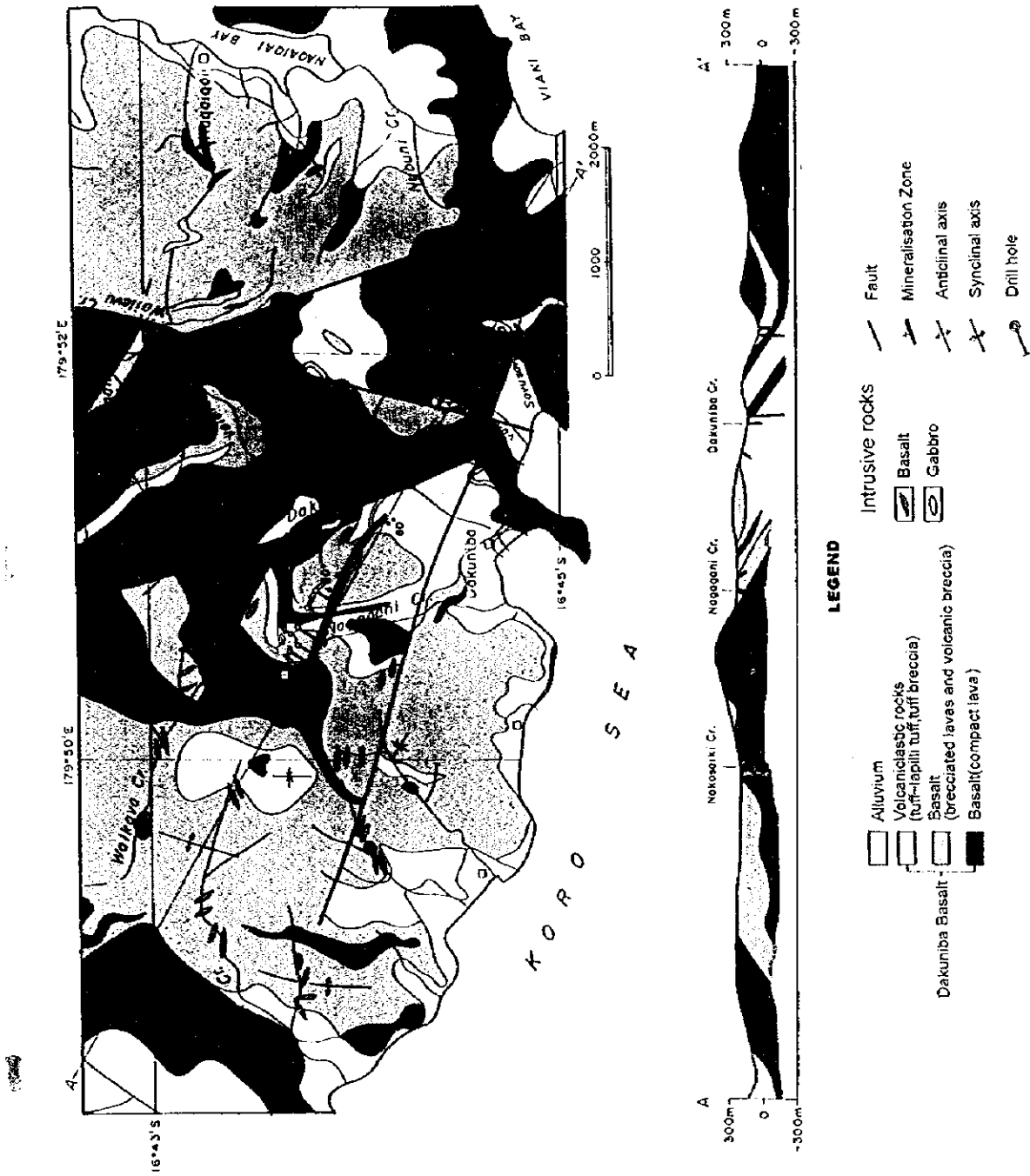
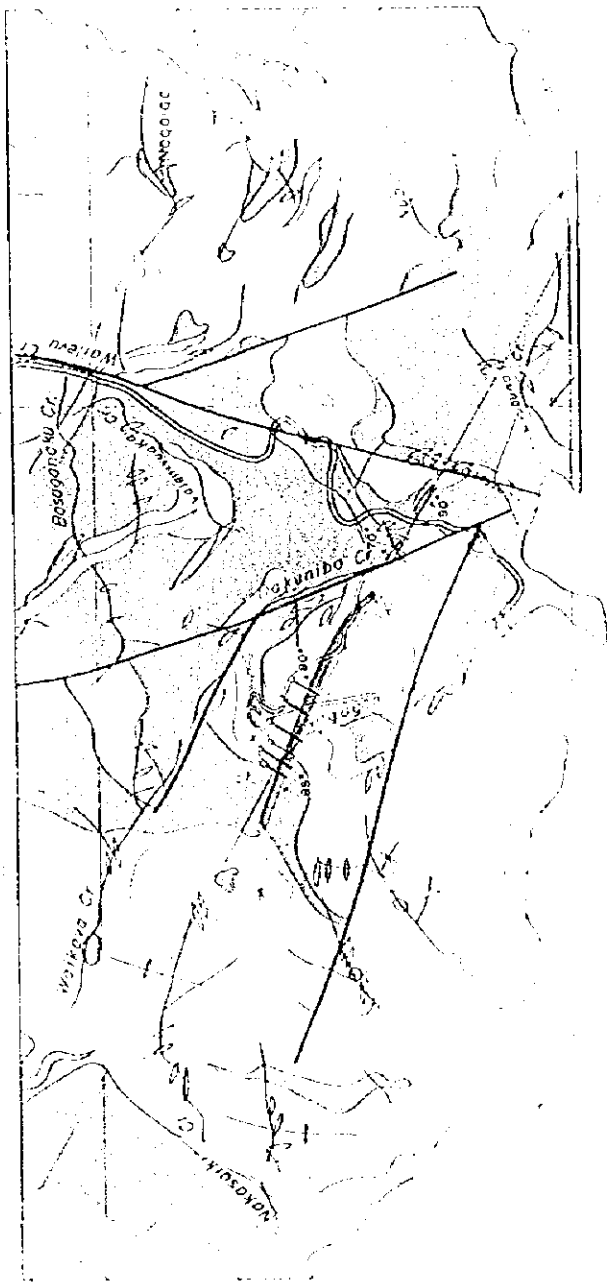


Fig. 1-9 Geologic Map of the Dakuniba Area



LEGEND



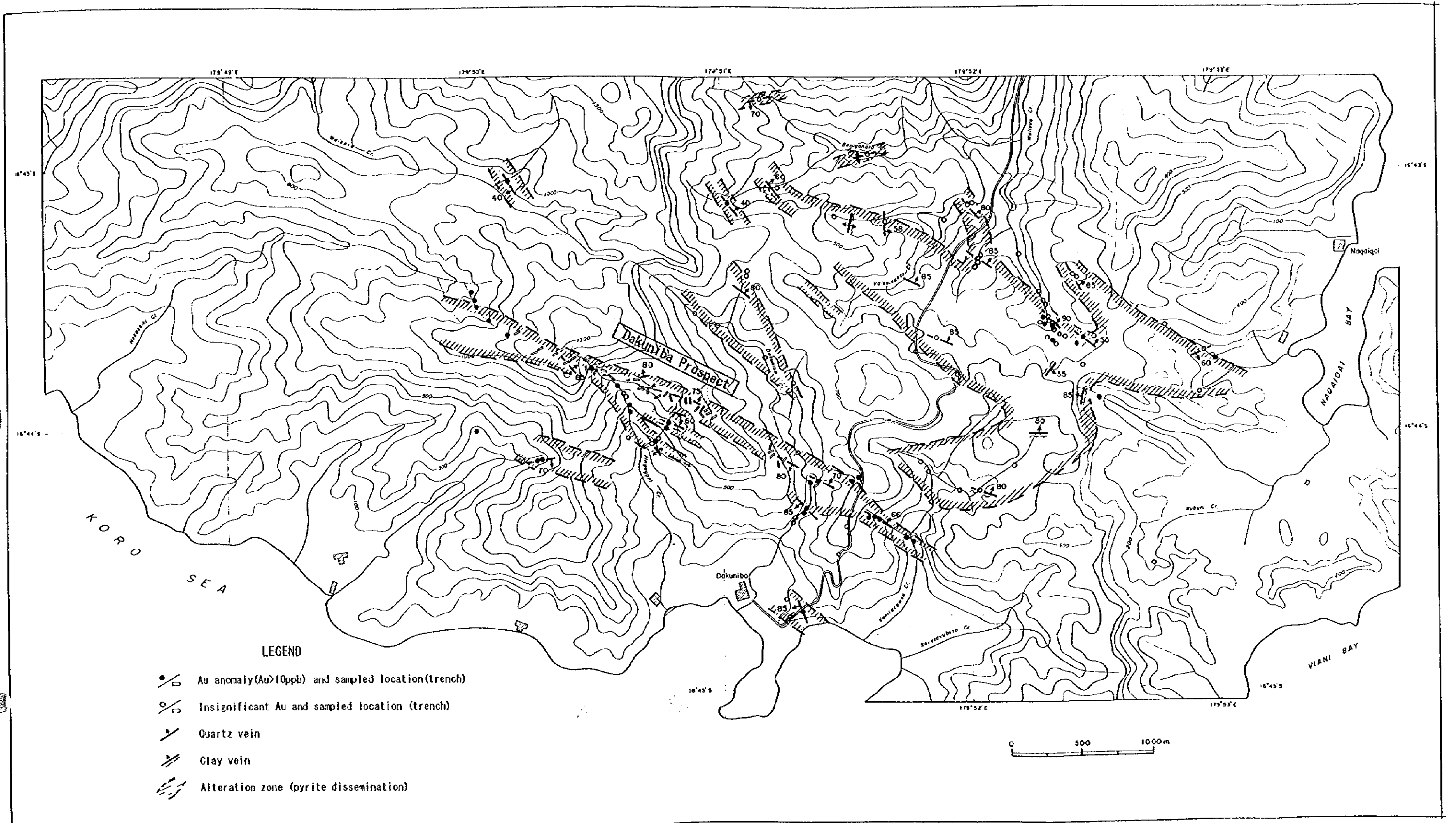


Fig. 1-10 Integrated Map of the Dakuniba Area

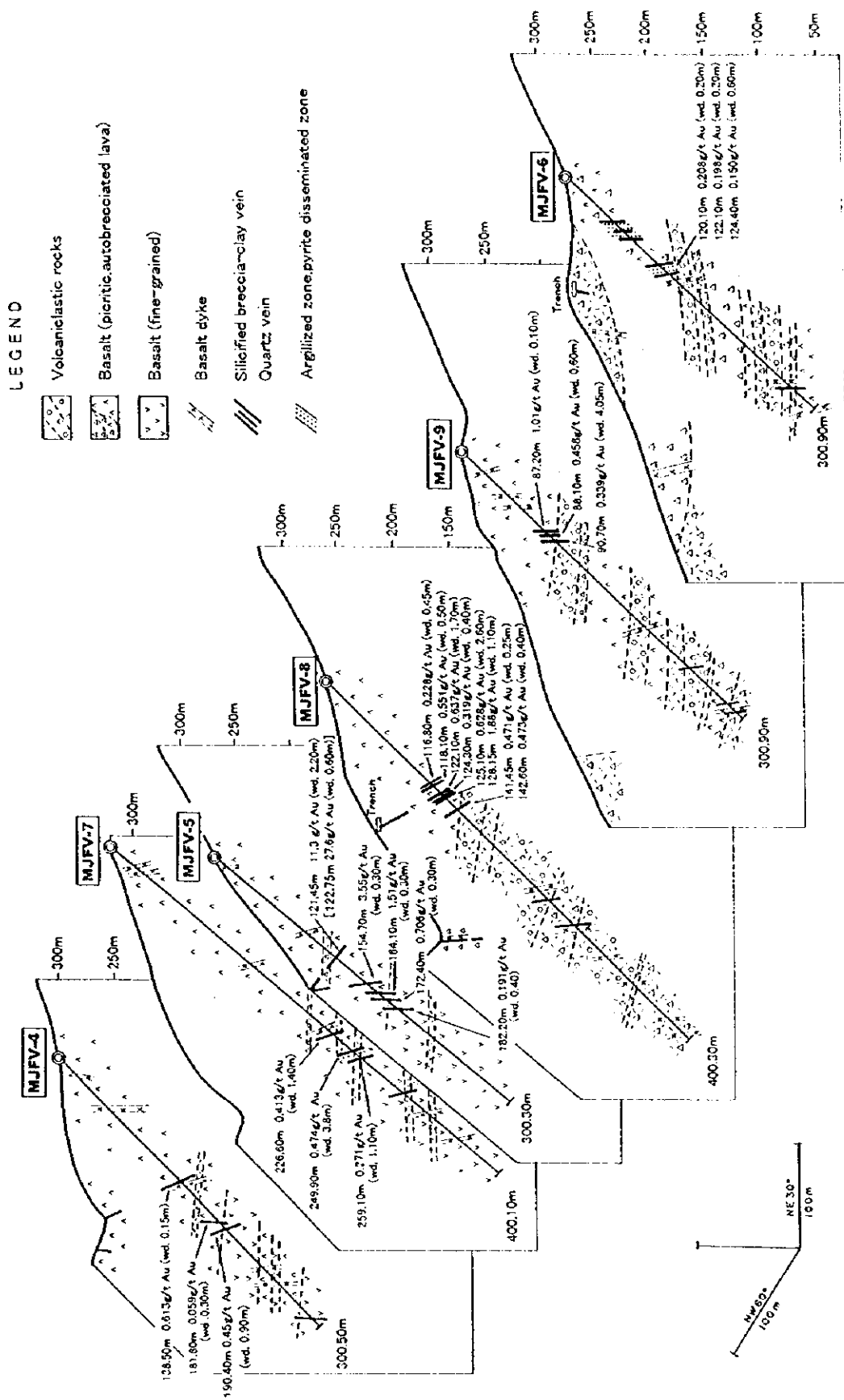
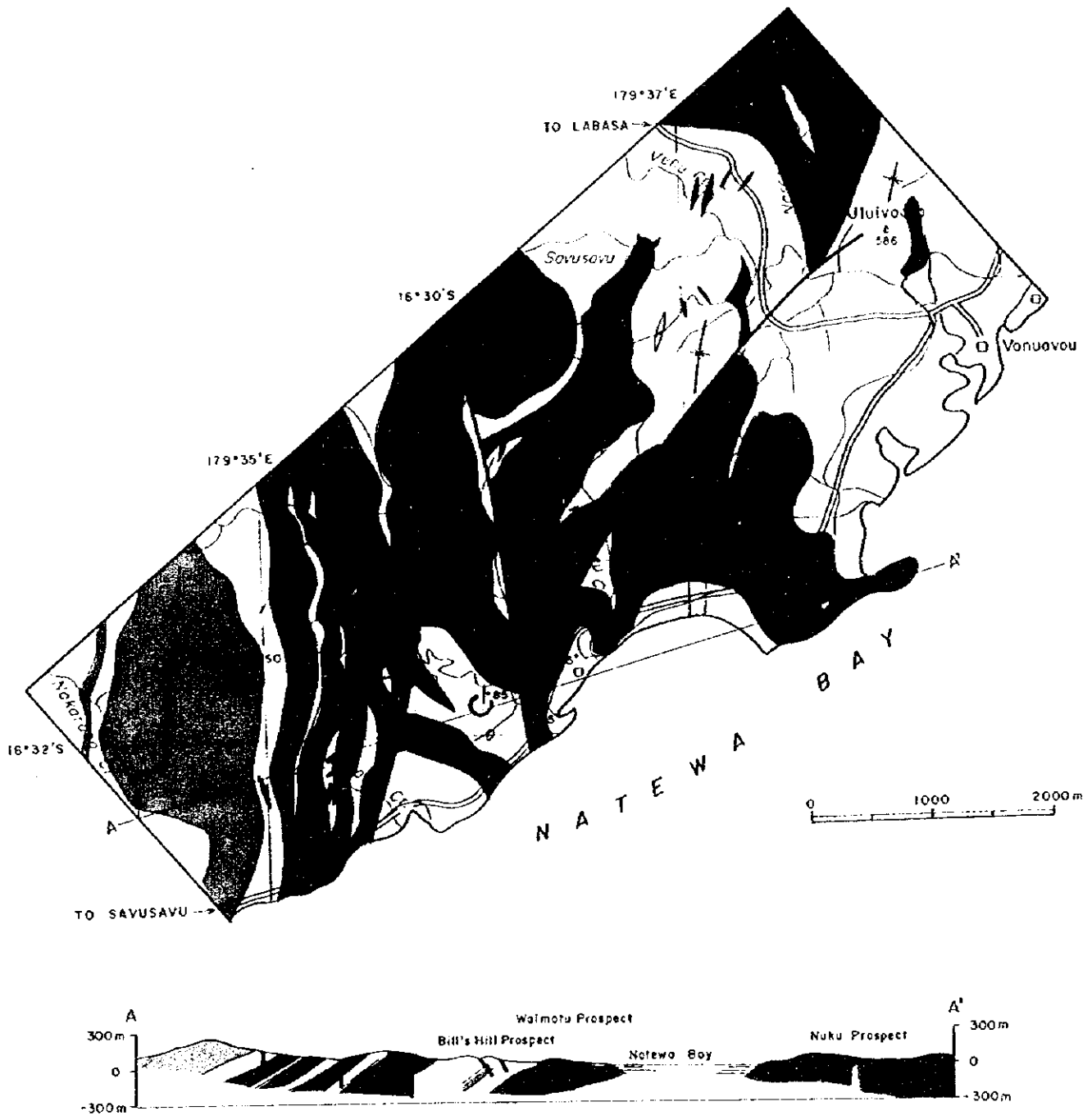


Fig. 1-11 Survey Results of the Dakuniba Area





LEGEND

<p>Korolini Breccias</p> <p>Koroutari Andesite</p>	<ul style="list-style-type: none"> Alluvium Volcaniclastic rocks Andesite lavas Basalt-andesite lavas Basalt lavas (propylitized) 	<p>Intrusive rocks</p> <ul style="list-style-type: none"> Andesite Quartz diorite porphyry Basalt Gabbro
	<ul style="list-style-type: none"> Fault Quartz vein/ stockwork Anticlinal axis Synclinal axis 	

Fig. 1-12 Geologic Map of the Waimotu Area

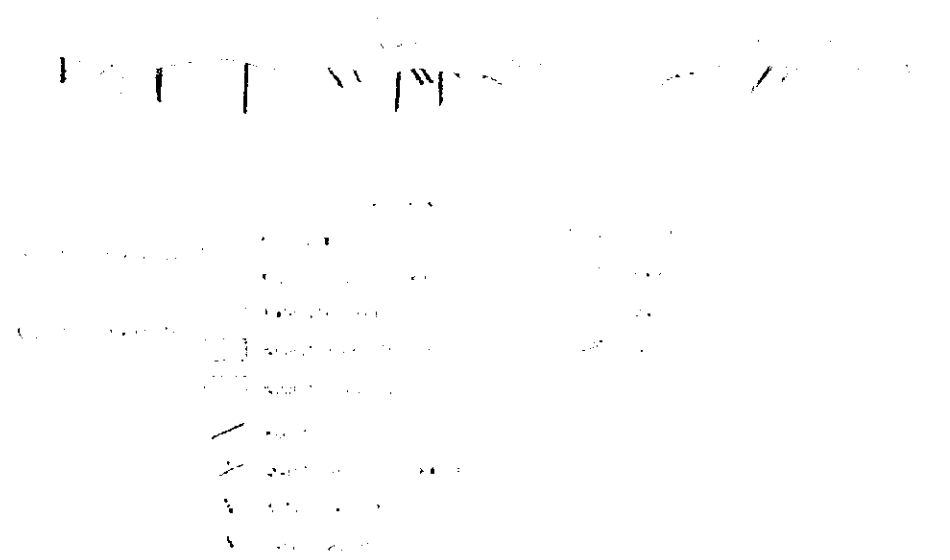


Fig. 1. Geological map of the region.

1

2

3

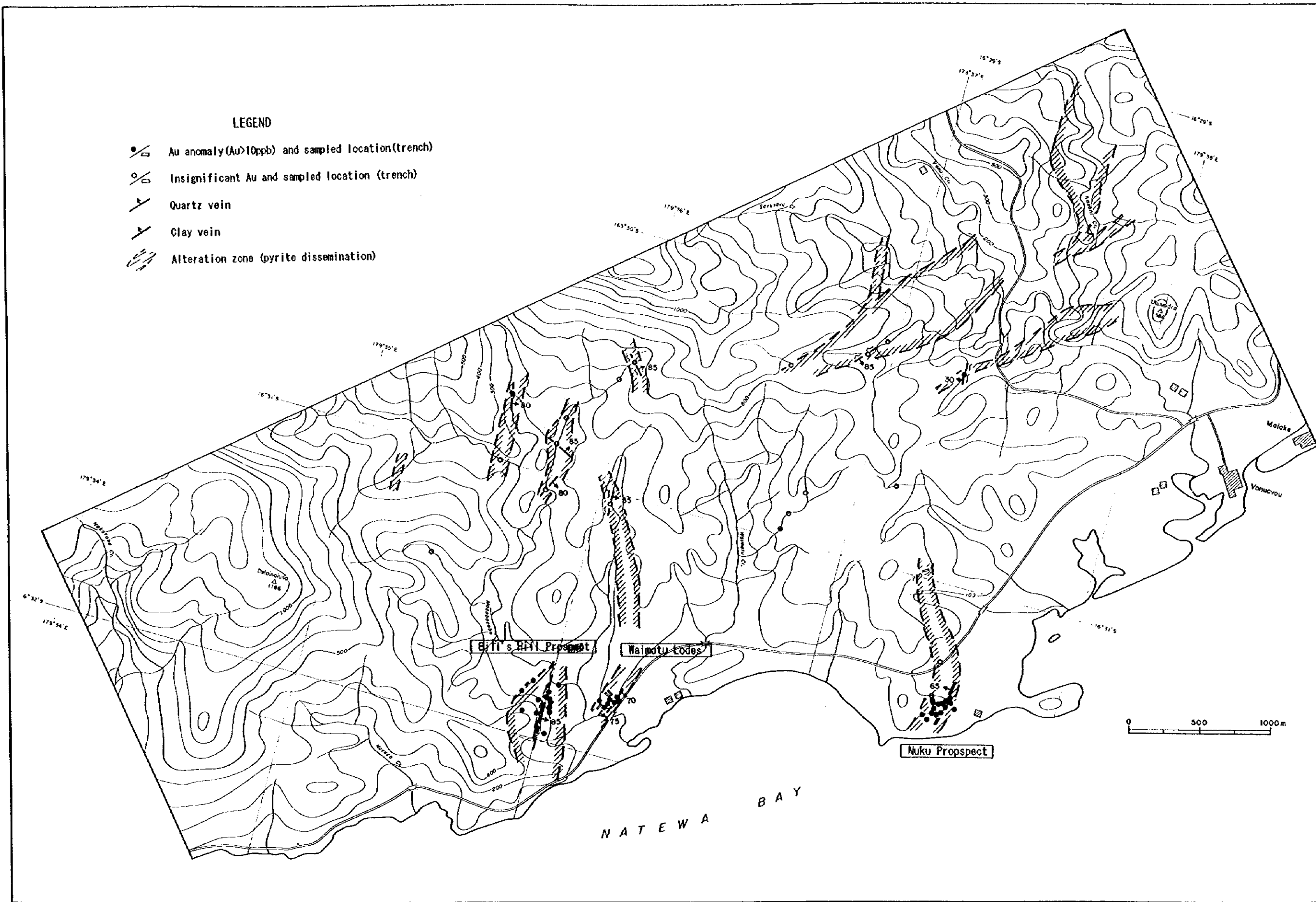


Fig. 1-13 Integrated Map of the Waimotu Area

PART II DETAILED DISCUSSION

PART II Detailed Discussions

Chapter 1 Compilation of Existing Data

1-1 Survey Method

Existing data consists of published scientific papers, geological maps by the Geological Survey and MRD, and reports from various companies. Most of them were available at the library of the MRD in Suva.

The main areas are the 57 prospects which are shown by Colley and Flint (1985). Firstly, twenty two prospects from the 57 prospects were selected by excluding existing tenements and bauxite deposits. Then reports on the 22 prospects were reviewed.

Criteria for screening the prospects are as follows.

Firstly, results of past exploration work and secondly, room for exploration. The criteria is what kind of exploration methods were conducted and what were the results, and whether the interpretation of the results was reasonable or not. The second is whether there exists the possibility that mineralization and alteration extend outside the prospect area, or not. It is difficult to evaluate the possibilities only from the report only, SLAR interpretation was applied for this purpose.

1-2 SLAR Imagery Interpretation

1-2-1 Outline

(1) Objectives

SLAR imagery interpretation was carried out in order to understand the regional geological structure and relationship with known prospects. This was used to help in the selection of geological survey areas.

(2) Area

The whole Vanua Levu island was selected for interpretation.

(3) SLAR imagery used

The imagery that are comprising of two different azimuths were provided by the MRD for interpretation as shown in Fig. 2-1-1. The characteristics of the imagery is as follows:

- | | |
|-----------------------|---|
| a. Wave length | 1.2 cm |
| b. Looking directions | northwestward: 11 strips
southeastward: 9 strips |
| c. Scale of imagery | 1:250 000 |

d. Mosaic prepared October 1984

(4) Method of interpretation

Regional photogeological interpretation was carried out. As a general geological interpretation had been conducted by Mallick and Habgood (1987), interpretation of the geological structures was emphasized during this work. The southeastward looked imagery is used for this work.

(5) Criteria for interpretation

The standards used for interpreting geologic structures are as follows.

a. Folds

Folds are identified by considering the distribution of geologic units, bends in the drainage pattern, trace of cuesta topography, extraction of strike ridges of the geologic units and other factors.

b. Lineaments

Lineaments indicate the existence of fractures on the surface or at shallow subsurface regions. Only those features considered to be geologically significant were extracted as lineaments. Those which are not clear are shown as broken lines on the map.

The major morphological features used for identifying lineaments are as follow.

- ① Existence of fault scarps
- ② Existence of linear fault valleys
- ③ Notably linear flow of rivers
- ④ Existence of kerncols and kernbutts
- ⑤ Linear continuation of break points of slopes

The above features vary in accordance with the geology, geologic structure and other factors of the area.

(3) Annular and dome structures

The morphological features for identifying annular structures;

- ① Inward radial or semi-inward radial drainage patterns
- ② Circular or arc shaped depressions with similar shaped marginal ridges.

In the structural feature mentioned in ②, it strongly suggests the existence of eroding calderas where there are sharp continuous scarps along the inner sides of the marginal ridges. These are called caldera structures (in the interpretation map, Fig. 2-1-1). Therefore, structures showing only first feature are called annular structure, in this work.

1-2-2 Interpretation of Geological Structure

(1) Folds.

a. Anticline: Existence of an east-west trending anticline is inferred near Mt. Bulebulewa in the northern part of the survey area. The length of the axis is about 15 km. This was based on the interpretation of morphology of ridges and the bedding trace on the eastern part of the south wing, although no bedding was traced in the northeastern part.

b. Syncline: Synclines are inferred at Dreketi River and Labasa River in the two areas near the center of the survey area. The syncline at Dreketi River is extending east-west and bedding traces are observed on both wings. The syncline around the Labasa River is also trending east-west, and its existence is shown by the interpretation of relatively lower topography though no bedding planes could be traced. These two synclinal structures are thought to represent a sedimentary basin of volcanoclastic rocks of the Natewa Volcanic Group.

(2) Lineament

A total of 171 lineaments were extracted from this area (Fig.2-1-2). The lineaments are most dense in the Udu Volcanic Area. Then, north of Savusavu, around Mt. Kasi and north of Dakuniba. The most prominent lineament runs from Labasa to Yasawa trending WNW-ESE with a total of about 450 km. It corresponds to the Nayarabale Fault (Colley and Greenbaum, 1980). The lineaments to the northeast of Nabouwalu where the Bua Volcanic Group is underlain are characteristic for their trends of N-S.

In the Area, 15 annular structures, 25 caldera structures and 8 dome structures are identified. These structures occur singly or form compound structures.

Structures	Number
Annular structure single	4
Caldera structures single	11
Dome structures single	4
Caldera & annular composed	10
Caldera & dome composed	3
Caldera, annular & dome composed	3

(3) Annular structures, caldera structures and dome structures

The largest caldera structure is located 15 km north of Labasa and has a 10 km diameter. The northern and the eastern of slopes of this structure are characteristic of a stratiform volcano. On the other hand, the southwest part is largely eroded and the volcanic structure is unclear. Within the caldera the Matailabasa and Coqeloa prospects are located.

The caldera structure surrounding the Mt. Kasi mine has a diameter of about 10 km. The Vakadrakara and Waidamudamu gold deposits are located here.

South of Koroinasolo in the western part of the island, a composite of annular and caldera structures are located. Within these structures the Nikoleisen prospect exists. East of the structure, there are three more caldera structures and within those hydrothermal alteration zones have been identified.

1-2-3 Interpretation of the Geological Structure

The Survey area is mainly underlain by volcanic rocks and the volcanic structures have not yet been identified and described except some of them. In this study, annular, caldera and dome structures are interpreted, and most of them may indicate centers of volcanic activities aligned on ENE-WSW, NE-SW and N-S directions. The alignment suggests fractures underneath the volcanoes.

On the other hand, geologic units are developed in zones around Naduri near Labasa and Cakaudrove Peninsula on the southeastern part of the island where neither annular, caldera nor dome structures are interpreted.. Table 2-1-1 including those zones showing volcanic and associated characteristics are tentatively named as volcanic zones.

The directional change of the volcanic groups may be attributed to a difference in the time of volcanic activity and faulting after eruption of the volcano.

The Seatura volcanic zone (2 in Fig. 2-1-4) corresponds to the Lomaiviti Trends (Colley, 1976) and is younger than the Nabua volcanic zone as suspected based on the well stratiformed morphology. The sense of the Lomaiviti Trend is right lateral. Therefore, Koroinasolo volcanic zone (1) and Nabua volcanic zone, now separated by the Seatura volcanic zone may have been a single volcanic zone. Leciaceva volcanic zone (5) trends oblique to the Dakuniba volcanic zone (7) and their time relations and formation are not clear. The Busaisau volcanic zone (8) and the Udu Trend (9) correspond to the Nayarabale Fault and are oblique to the Nabua volcanic zone in the south and parallel to the Dakuniba volcanic zone.

The major prospects and hydrothermal alteration zones and gold deposits are located within the volcanic zones.

Table 2-1-1 Volcanic Zones in Vanua Levu

Trend	Major Trend (Volcanic zone)	Direction	Length of Zone (km)	Width of Zone (km)	Number of Annular, Caldera, Dome structure	Main Prospect	No. in Fig. 2-1-4
ENE-WSW	Koroinasolo	N70° E	25	7.5	6	Nikoleisen Koroinasolo	①
	Naduri	N75° E	30	7.5	1		③
	Nabua	N70° E	88	15	10	Mt.Kasi Lomaloma Waisali Waimotu/Nuku	④
	Lesiaceva	N80° E	25	5	-	Savudrodoro	⑤
NE-SW	Cakaudrove	N50° E	510	7.5	2	-	⑥
	Dakuniba	N45° E	5+	10	2	Dakuniba	⑦
	Bucaisau	N55° E	45	10	2	Matailabasa Coqeloa Wainikoro Mouta Nubu	⑧
	Udu	N55° E	55	15	1	Udu	⑨
N-S	Seatura	N	30	10	5		②

1-3 Selection of Geological Survey Areas

1-3-1 Outline

The existing data on the prospects outlined above were reviewed based on the following criteria.

- a. Areas where alteration is known will be selected if:
- the size of the alteration area is large,
 - mineralization is not sporadic
 - structures (faults) with known mineralization exist,

- geochemical anomaly is large, and
- high gold values are found.

b. Areas among the above where past exploration work has not been sufficient compared to the size of mineralization and alteration zone or geochemical anomaly, and where drilling should prove the potential of gold mineralization.

From the results, prospects near Mt. Kasi, porphyry type-epithermal type prospects near Koroinasolo, Kuroko type prospects near Wainikoro, gold prospects near Nakoroutari, prospects near the Waimotu Lodes, and the Dakuniba Prospect were thought most promising. The former three areas were within existing tenements at the time this study. The latter three are left for the Geological Survey.

1-3-2 Nakoroutari Area

(1) Location

15 km south of Labasa

(2) Commodities

Au, Ag

(3) Geology and mineralization

Mineralization occurs in andesitic lavas and volcanoclastic rocks and conglomerate, sandstone, and mudstone. Quartz veins and breccia zones are controlled by faults. The geochemical survey area is called Leli's Prospect. In a 700 m × 200 m area, float with quartz veins and/or pyrite dissemination is widespread and the highest value was 7.9 g/tAu. Native gold, chalcopyrite and sphalerite occur in the breccia zone along the faults. The homogenization temperatures of fluid inclusions range from 184°C to 204°C.

(4) Previous work conducted

Since 1988, PacAu (Fiji) Ltd. and Paget Gold Mining (Fiji) Ltd. conducted the following survey within SPL1301.

- Geochemical Survey

Creek sediment samples: 60 pcs

Rock chip samples: 161 pcs

Soil samples: grid sampling, 400 m × 500 m

- Diamond drill holes

6 holes, 1,053 m total length

(5) Previous work results

The highest value from the fault breccia zone is 17.9 g/tAu. Samples taken over 600 m averages 4.7 g/tAu and 33 g/t Ag. The highest value from core samples was 11.6 g/tAu over 0.6 m intervals.

(6) Room for exploration

The survey was conducted over a narrow area of 700 m N-S by 600 m E-W. The mineralization zone crops out along Korobua fault zone intermittently over 600 m.

The maximum length of individual exposures is about 80 m. The area of north of the Leli's prospect is gently undulating and sugar cane fields are developed, so that exposure of rocks is poor. As the area increases in elevation toward the south, exposure tends to be better but existing data does not show details of alteration and mineralization. An interesting feature is a half caldera structure interpreted from the SLAR imagery.

In conclusion, it is certain that gold mineralization occurs around Leli's Prospect and geologic structures that may control the gold mineralization are developed. The mineralization with significant gold values and the geologic structure presumably preferable for circulation of ore solution indicate this has a potential for gold emplacement good enough to conduct Geological Survey.

1-3-3 Dakuniba Area

(1) Location

The area is located 65km east of Savusavu.

(2) Commodities

Au, Ag

(3) Geology and mineralization

Mineralization occurs in andesitic rocks of the Natewa Volcanic Group, and is emplaced in quartz veins and breccia zones that are controlled by the faults. Major alteration extends in a WNW-ESE direction over 4km. Ore minerals are chalcopyrite, marcasite, galena, sphalerite, arsenopyrite and barite.

(4) Previous exploration work conducted

This area has been explored since 1930. In 1957 the Geological Survey drilled two holes totaling 176 m in length after rock chip samples returned 13 g/tAu. In 1969-1971, Barringer took 378 Creek sediment samples and outlined a weak Cu anomaly (cold extractable). Since 1986 Pacific Islands conducted geochemical surveys by soil and rock chip samples, trenching and CSAMT survey. No drilling was conducted.

(5) Results of previous work

As a result of a geochemical survey, a weak soil anomaly (more than 10 ppb) was outlined over 1km north of Dakuniba village. Trenching was done extensively on and around the area. The highest value from the trenches was 12.8 g/tAu over 1.5 m width. The low grade gold zone less than 1 g/tAu extends over

3.2km.

(6) Room for survey

Geochemical anomalies are widespread. This area is thought to be a prospect that had not been properly drilled before. Therefore this area has a high potential for gold deposit emplacement and is selected as a Geological Survey Area.

1-3-4 Waimotu Area

(1) Location

Here, the Waimotu Area is defined as the area including the Waimotu Lodes, the Bill's Hill prospect and the Nuku prospect. Bill's Hill is 65km from Savusavu. The Nuku prospect and Waimotu Lodes are located 0.5km and 2.5km east-northeast of Bill's Hill, respectively.

(2) Commodities

Au, Ag

(3) Geology and mineralization

This area is underlain mainly by basaltic andesite rocks with locally intercalated volcanic breccia. Waimotu veins show echelon-like alignment consisting of N-S trending chalcedony-quartz. The grades range between 7-22 g/tAu and 5 g/t Ag. Seven diamond drill holes were aimed at lower extensions of the veins. The 40 m strike lengths does not seem to improve. At Bill's Hill silicified and argillic (kaolinized) zones grade 0.2-0.5 g/tAu. A lower stockwork zone grades 0.4 g/tAu. At the Nuku Prospect, a breccia zone containing chalcedony-quartz veins has developed. Outcrop grades 5.6 g/tAu over 4.5 m.

(4) Previous exploration

1938	Waimotu Lode was discovered.
1940-42	Emperor drifted tunnels for 551 m and drilled 7 holes totaling 609 m.
1974-?	Jennings conducted soil geochemical survey. Other companies, Aquitaine, BHP, Consolidated Goldfields, J/V of Moninex, Goldfields and Canyon Resources, J/V of GeoPacific and Delta Gold NL conducted exploration work including soil sampling, pitting and trenching.

(5) Results of exploration work

At the Waimotu Lode three holes intercepted a mineralization zone out of seven holes. The best intercepts were 17.9 g/tAu over a 0.6 m interval. At Bill's Hill, 8 holes totaling 846 m were drilled. Three

holes intercepted mineralization with the best assay of 4.3 g/tAu over 0.6 m. At Nuku, 4 holes totaling 310 m were drilled with a best result of 0.46 g/tAu over 9 m intervals.

Hole No.	Azimuth	Inclination	Length	Intercept		
				Depth(m)	Interval(m)	Assay Results(g/tAu)
BH85-1	82	-45°	150.3	36.0	14	1.2
BH85-2	85	-70°	192.1	12.0	6	1.2
BH87-3	-	-90°	51.1	25.9	1.2	1.5
BH87-4	-	-90°	64.6	37.0	12.2	0.27
BH87-5	-	-90°	50.2	4.8	21.8	0.77
BH87-6	-	-90°	35.7	25.3	2.1	0.86
BH87-7	-	-90°	40.3	29.1	7.1	0.17
BH87-8	85	-54°	261.75	101.1	0.6	4.3

Assay results from the quartz stockwork zone near the collar of DDH-1 was 7.2 g/tAu over a 1 m interval. The grade of the stratiform silicified breccia zone ranges from 0.2 to 0.5 g/tAu.

The Waimotu Lodes were explored and developed during 1940-41. In 1949, prospectors sampled from costeans and the results were as follows:

Lode	Strike length (m)	Average width (m)	Average grade (g/tAu)
East Lode	33	0.8	11
Main Lode	34	0.7	17
West Lode	18	0.2	17

In 1941, the best result from the Emperor's drilling was 2 m @ 9.9 g/tAu within 14 m @ 1.2 g/tAu. Two other interceptions were only less than 1.5 g/tAu. The total proven reserves was 5,480 t of ore with a grade of 9.9 g/tAu with an average of 0.43 m.

At Nuku, the average grade of chalcedonic quartz veins was 1.3 g/tAu at trenches. The best assay was 13.5 g/tAu over 1.5 m interval. The results of drilling were disappointing because of the low grade.

(6) Room for exploration

The previous work conducted was limited to three prospects and the surrounding area was not surveyed extensively. Existing data does not show the mineralization and alteration in the surrounding zone. On the other hand, a lineament that corresponds to the Nayarabale Fault and a caldera structure were interpreted by SLAR Imagery north of the three prospects. It is noteworthy that the Yasawa prospect is located near the intersection of the two geologic structures. In this area gold prospects are relatively

densely distributed and the downward extension of these areas was not sufficiently explored. Therefore, the area including the three prospects is selected for the Geological Survey Area.

Chapter 2 Nakoroutari Area

2-1 Geological Survey

2-1-1 General Geology

Mineralization occurs as quartz veins and breccia zones (fault breccia) in the Koroutari Andesites of the Natewa Volcanic Group. Four mineralization and alteration zones are distributed in this area. However, High gold values are limited to the Leli's prospect.

The mineralization of the area is considered to be of epithermal origin based on crustification texture of the chalcedonic quartz veins with small amounts of chalcopyrite and sphalerite and minor element contents in the veins at Leli's Prospect. The mineralization may be classified into low sulfidation type judging from the alteration zone that may be related to mineralization in narrow quartz veins containing minor amounts of sulfide. Previous drilling revealed abundant shear zones developed underneath this area.

2-1-2 Stratigraphy

The Natewa Volcanic Group in this area is divided into three formations: the Koroutari Andesites, the Sueni Breccias and the Wailevu Formation.

(1) Koroutari Andesites

The Koroutari Andesites are distributed widely under this area and consist of andesite lava, basalt lava and coarse volcanoclastic breccia. The lavas do not display a clear pillow texture, presumably they were erupted on land and flew into the shallow sea. Ibbotson (1969) estimated 70% of the constituents are volcanoclastic. On the geological map this formation is divided into three mappable units: a basaltic lava dominant member, andesite-basaltic andesite lava dominant member and a volcanoclastic facies dominant member.

Basalt lava is distributed in the northern and southwestern part of the area. The unit in the northern part is blackish in color and consists of auto-brecciated and weakly compact lavas.

The andesite to basaltic andesite lava unit is widely distributed in the area. It is blackish to dark green. Sometimes it is difficult to distinguish it from the above andesite lava unit, but it has less mafic phenocrysts, paler in color and sometimes porphyritic. The unit is massive, and it sometimes may be auto-brecciated to hyaloclastite facies.

The volcanoclastic unit consists mainly of lapilli tuff but fine tuff is dominant in the north and east. Mudflow facies in the unit is distributed in the north.

These units are considered to be correlated to the relatively lower part of the Natewa Volcanic Group. The Wailevu Formation of Ibbotson (1969) is distributed in the northwestern part of the area. In this study the Wailevu formation is included in the volcanoclastic unit of Koroutari Andesites in this survey. Ibbotson (1969) indicates the Wailevu Formation consists of epiclastic sediments: grit, sandstone, sandstone and minor amounts of graywacke and breccia.

The Maximum thickness of the Koroutari Andesites is estimated at 300 m. Ibbotson (1969) estimates the maximum thickness of the Koroutari Andesites is at 450 m.

(2) Sueni Breccia

This formation is mainly distributed in the southwestern part of the high lands in the area. It consists mainly of hyaloclastic volcanic breccia and of finer grained volcanoclastic breccia deposited in a shallow marine environment. It is grayish to blackish in color and generally lacks bedding, except along the fine tuffs.

Ibbotson (1969) indicates the Sueni Breccias and Koroutari Andesites are the same age. However, in this survey they are mapped as the Sueni Breccias overlying the Koroutari Andesites unconformably, while the true relationship between both formations is not observed. This formation tends to be distributed at higher elevation, and has not undergone significant alteration.

The Maximum thickness of the Sueni Breccias is estimated at 400 m.

2-1-3 Intrusive Rocks

Basaltic rocks are intruded in many places within the area. The widths of dykes are generally 1 m to 5 m. The dominant trend is N-S and NW-SE. Phenocrysts include olivine, clinopyroxene and plagioclase, in a groundmass consisting of fine-grained clinopyroxene and plagioclase. They have undergone weak alteration with olivine being replaced by smectite.

2-1-4 Geologic Structure

The most prominent geologic features are N-E to NNE-SSW trending faults and NW-SE faults. The western block in Leli's prospect in the central part of the area is down-thrown in the east. The Korobua fault zone is a series of faults running N-S around the Korobua Creek and Saquru Creek area.

The volcanoclastic layers that are distributed in the northwest show ENE-WSW strikes and dip 15 °N. The volcanoclastic rocks in the northeast strike E-W and dip 15°N.

The intercalation of volcanoclastic layers in the Drakaniwai Creek area in the south strike E-W to NW-

SE and dip 30°N. Between the two areas, a small anticline and syncline exist.

2-1-5 Mineralization and Alteration

(1) Leli's Prospect

At this prospect, silicification occurs along the Korobua fault. In trenches, silicified breccias are distributed in the matrix of the volcanoclastic rocks. The silicified zone along the Korobua fault contains quartz veins emplaced within a shear zone in andesitic lapilli tuff. Quartz veins carry a small amount of sulfides: pyrite, chalcopyrite, and galena. Quartz veins consists of fine-grained zones and medium grained zones showing crustification texture. Early fine-grained chalcedony is cut later by a quartz vein. Quartz precipitation and brecciation proceeded repeatedly.

Microscopic observation indicates that quartz fragments and matrix are replaced by quartz and sericite (or sericite-smectite mixed layer mineral). Barite is observed in three samples that are from the east breccia zone. They accompany quartz and iron oxide (goethite and hematite).

(2) South of Leli's Prospect

About 1 km south of the junction of the Wairikicake and Wairikiqisi Rivers, small areas of alteration and silicification have developed and quartz veinlets occur in weathered porphyritic andesite at two localities. They trend NNW-SSE to NW-SE with a vertical dip. The assay results are 0.30 g/tAu (width 5 cm) and 0.55 g/tAu (width 0.10 m). The andesite that has undergone propylitic alteration with pyrite dissemination over 400 m trends in an N-S direction.

(3) Mugsy's Prospect

An argillic alteration zone is developed at the Navaka Creek. Exposure around this area is very poor and an N-S trending fault is suspected from the aerial photographs. Gold values are 0.01 g/t or less, while As (maximum 90 ppm) and Hg (0.388 ppm) are anomalous. It appears hydrothermal alteration has taken place with accompanying mineralization.

(4) Navakuru Prospect

Silicified floats with pyritization are distributed from the Sueni village to the Navakuru village. A quartz vein bearing pyrite of 20 cm width strikes N78°E and dips 65°S. However, assay results of Au, Ag and Sb were below the detection limits, and As and Hg are as low as 6 ppm and 112 ppb, respectively. The highest value in this area is 0.02 g/tAu from a limonitic vein.

2-2 Geochemical Survey

2-2-1 Method

A total of 189 samples were submitted for chemical analysis. The basic statistics are as follows (also see Figs. 2-2-6,-7 and -8). The statistical analysis was done after logarithmic conversion was made.

2-2-2 Assay results and Basic Statistic Data

Au: 60% of samples are below detection limit (<0.01g/t). The samples that grade more than the detection limit indicate that they have undergone some kind of mineralization. The cumulative frequency curve indicates the samples above detection limit consist of two groups. The numbers of samples that are higher than (average + σ) and (average+2 \times σ) are 15% and 7% of the total. Judging that the samples were taken from quartz veins and altered rocks, the values may be too high for thresholds. Therefore, 0.01 g/tAu and 0.08 g/tAu are used for the thresholds to delineate anomalous zones (Figs. 2-2-9 and -10).

Ag: 0.04 g/t(detection limit) and 3.1 g/t (average+2 \times σ) are selected for threshold.

As: 15 ppm (average + σ) and 90 ppm (average+2 \times σ) are selected for thresholds.

Sb: 0.5 ppm (detection limit) and 1.6 ppm (average+2 \times σ) are selected for threshold.

Hg: 0.09 ppm (average + σ) and 0.24 ppm (average+2 \times σ) are selected for thresholds.

The correlations between two elements are shown in the table below and correlation graphs at the end of Chapter Four. Au does not appear to be correlated with Ag, As, Sb or Hg. On the other hand, Ag has clear correlation with As and Sb.

Element(unit)	Au(g/t)	Ag(g/t)	As(ppm)	Sb(ppm)	Hg(ppm)
Detection Limit	0.01	0.4	1.0	0.5	0.005
Average	0.014	0.4	2.6	0.36	0.037
Minimum	<0.01	<0.4	<1.0	0.25	0.007
Maximum	12.9	14.9	210	14.3	92
Average + σ	0.08	1.1	15	0.77	0.091
Average+2 \times σ	0.45	3.1	90	1.6	0.24

	Ag	As	Sb	Hg
Au	0.28	0.31	0.09	0.01
Ag		0.57	0.64	0.28
As			0.68	0.36
Sb				0.38

The correlation between Au and the other four elements is obvious. The correlations among the other four elements are admitted.

2-3 Geophysical Survey (Array CSAMT and Time Domain IP Methods)

2-3-1 Outline of Geophysical Survey

(1) Survey method

To clarify the relation between the subsurface structure and resistivity in the Nakoroutari zone, which is selected by previous surveys and the present geological survey, by Array CSAMT method and also to understand the relation between the CSAMT anomalies and mineralization by Time Domain IP(TDIP) method. Geophysical anomalies will be extracted at the same time in order to obtain guidance for drilling exploration.

Eight profiles totaling 12,000 m and 120 stations were measured with the array method. With the IP method, for the resistivity anomalous area selected by CSAMT, five profiles totaling 7,500 m were measured (Figs. 2-2-11, and -12). The lengths of traverse lines and the numbers of stations are as follows.

Array CSAMT Method				Time Domain IP Method			
Line	Length (m)	Number of stations	Station interval(m)	Line	Length (m)	Number of stations	Station interval(m)
A	1,500	15	100				
B	1,500	15	100	B	1,500	55	100
C	1,500	15	100	C	1,500	55	100
D	1,500	15	100	D	1,500	55	100
E	1,500	15	100	E	1,500	55	100
F	1,500	15	100	F	1,500	55	100
G	1,500	15	100				
H	1,500	15	100				
Total	12,000	120			7,500	275	Total

* Line interval: 200 m

2-3-2 Array CSAMT Method

(1) Selection of Traverse Lines

The analysis and interpretation of the reports of previous surveys indicated that the strike of the regional structure in the Nakoroutari Zone is N-S-NW-SE. In order to clarify the resistivity structure of the Leli's prospect of the survey area and to pursue the relation between geological structure and mineralization, eight CSAMT lines at 200 m intervals transecting the silicified zone at N72° E direction were measured (Fig.2-2-12).

(2) Field Operation and Equipment.

The standard configuration is four Ex dipoles and one Hy magnetic field measurements for each of the 12 frequencies, The Ex fields are measured with a dipole using non-polarizable porous pots. The survey traverse line, for the series of equally spaced Ex dipoles, is parallel to the transmitter dipole. A horizontal magnetic sensor coil is placed on the ground, approximately at the center of the series of Ex field. It must be placed several meters away from the Ex dipole line and the receiver console, to avoid interference.

The measurements are performed at each of twelve frequencies with a binary step: 4,8,16, 32,64,128,256,512,1024,2048,4096 and 8192 Hz, and are three time operations to make sure the repeatability of data.

The equipment manufactured by Zonge in USA is shown Fig. 2-2-13 for field configuration and in Table 2-2-1. The transmitter (powered by a suitable motor generator) sends current into the grounded dipole (distance of two electrodes is about 1500 m), shown in Fig. 2-2-11, located 7 km NW from

Nakoroutari Area.

The transmitting dipole is at a distance of about 1.5 km in the N72° E direction. The coordinates and conditions are as follows:

	Location	Elevation(m)	Orientation of dipole	Distance of Dipoles	Current (Amp)
A electrode	Lat. 16° 28'55"S Long. 179° 21'55"E	24	N72° E	1,500 m	12 (Max.)
B electrode	Lat. 16° 28'50"S Long. 179° 22'25"E	27			

The field conditions of random stations were the same as array system on the survey line with the exception of measurement of one Ex field.

(3) Data Processing and Interpretation

The magnitudes of Ex and Hy are measured at the stations, the resistivities and the parameters (the phase differences in Ex-Hy and the standard deviation) are calculated, stored in the RAM of the receiver unit and transferred into the field personal computer at the end of each day. The data were immediately processed at the camp. The field presentation of the results is in the form of a contoured apparent resistivity pseudo-section plot and a plane map. The skin depth equation suggests that the data of lower frequencies inform us of deeper characteristics, the CSAMT data can be plotted with frequency as the sounding parameter (vertical axis) and receiver position as the lateral parameter (horizontal axis). This type of plot is called a sounding pseudo-section, and the plane maps of each frequency are plotted with the apparent resistivity.

Table 2-2-1 Equipment for CSAMT Method

Item	Model	Specification	Quantity
Transmitting system	Chiba Electric Transmitter CH-120A	Output Voltage : 400,600,800,1000V Output Current : 0.1 - 20A Wave Form : Rectangular wave Frequency : DC - 8,192 Hz Weight : 40 kg	1 pc.
	Zonge GGT-20 Transmitter	Output Voltage : 400,600,800,1000V Output Current : 0.4 - 40A Wave Form : Rectangular Frequency : DC - 8,192Hz Weight : 120 kg	1 pc.
	Zonge XMT-16 Transmitter Controller	Frequency : DC-8,192Hz Weight : 5.8 kg Power Requirement : 12 Volt Battery	1 pc.
	Zonge ZMG-20 Engine Generator	Maximum Power : 20 kW Frequency : 400 Hz Output Voltage : 115V Power : 62Hp	1 pc.
Receiving System	Zonge GDP-16/8 Data Processor	Input Channel : 0.03 μ V Sensitivity : 8 ch Weight : 23 kg Power Requirement : DC 12 Volt	1 pc.
	Zonge ANT/1B Antenna	1 Coil Weight : 6.2 kg	1 pc.
	Electrode Current Potential	Fe Plate : 24cmx36cm Non-polarizable : CuSO ₄ Porous Pot	30 sheets 6 pcs

One-Dimensional Inversion Analysis

The CSAMT curve, plotted with twelve frequencies as X-axis and apparent resistivity as Y-axis, is interpreted for one-dimensional multi-layer structure by computer(Fig. 2-2-14).

Two-dimensional Inversion Analysis

There are two methods of two-dimensional analysis, one is called forward method, and the suitable model made from the result of one-dimensional analysis is calculated. The other is called inversion method; the fitness model is obtained directly from observed values. In this report, two-dimension inversion analysis is applied for the CSAMT anomaly zones. The program was prepared by Ogawa and Uchida (1988, GSJ). This program calculates the coefficients of partial differential equation for the parameters of

response function when the model is calculated by forward method. The second step is that new parameters are set by the inversion analysis applied numerical solution of singular value. The most fit model of minimum deviation with observed values is selected from these parameters.

2-3-3 Time Domain IP Method

(1) Field Operation and Equipment

a. Method of measurement

The method of TDIP measurement in the field is as follows: the five receiving dipoles and transmitting dipole are set on the survey line as shown in Fig.2-2-15.

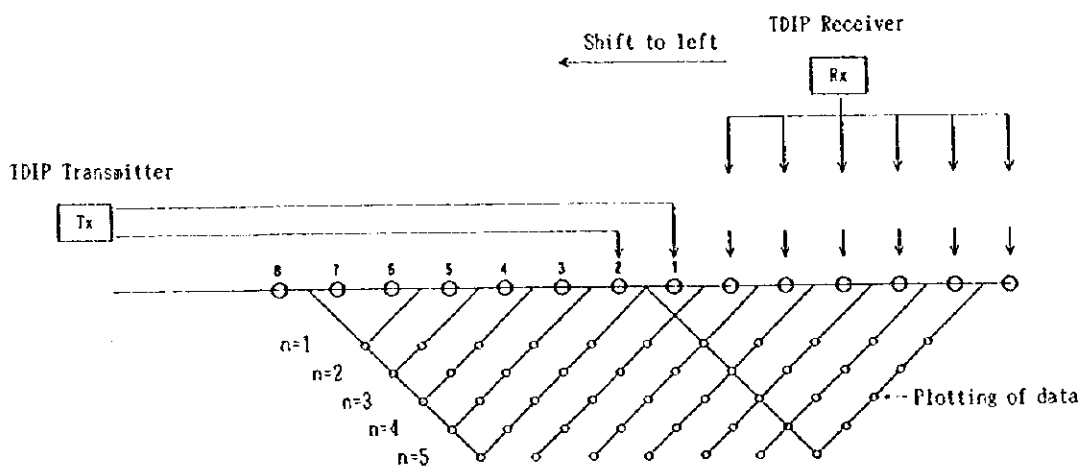


Fig. 2-2-15 Survey Configuration of IP Method

The specification of IP survey is as follows.

- The configuration of electrode array : dipole-dipole
- The separation of electrode : 100 m
- The coefficient of electrode separation : n=1-5
- The duty cycle of on/off time : 2 sec.

b. The equipment for TDIP survey

The equipment used in this survey is listed in Table 2-2-2.

(2) Data Processing and Interpretation

The measured resistivity and chargeability values are shown in tables for each line on the profiles. The

subsurface depths are shown on plane maps by the electrode separation index. And the subsurface electric characteristics can be understood from these plane maps and profiles.

The resistivity values were affected by the topography and thus terrain correction was made by using carbon paper.

Two-dimensional model simulation was carried out for IP anomalies and chargeability and resistivity values were obtained quantitatively for the anomaly sources.

Table 2-2-2 Equipment for TDIP Method

Item	Model	Specification	Quantity
Transmitting system	Zonge GGT-20 Transmitter	Output Voltage : 400,600,800,1000V Output Current : 0.4 - 40A Wave Form : Rectangular Frequency : DC - 8,192Hz Weight : 120 kg	1 pc.
	Zonge XMT-16 Transmitter Controller	Frequency : DC-8,192Hz Weight : 5.8 kg Power Requirement : 12 Volt Battery	1 pc.
	Zonge ZMG-20 Engine Generator	Maximum Power : 20 kW Frequency : 400 Hz Output Voltage : 115V Power : 62Hp	1 pc.
Receiving System	Zonge GDP-16/8 Data Processor	Input Channel : 0.03 μ V Sensitivity : 8 channel Weight : 23 kg Power Requirement : DC 12 Volt	1 pc.
Electrode	Current Potential	Stainless steel rod : 0.6 cm ϕ x60 cm(L)	10 pcs
		Non-polarizable : CuSO ₄ Porous Pot	6 pcs

2-3-4 Results of Array CSAMT Method

(1) Outline of the results

The apparent resistivity ranges from 0.9 to 168 ohm-m. Areas of low resistivity prevail and background values are low at 15 to 25 ohm-m. The area over 50 ohm-m is deemed to be of high resistivity and less than 10 ohm-m is of low resistivity.

(2) Sections of apparent resistivity

Fig.2-2-16 shows resistivities from surface to depths that correspond with high- to low-frequency.

Line A. High resistivity of intrusive rocks are delineated by discontinuance of stratiform contours which indicate sudden changes in resistivity between Nos.6 and 8 in the middle of the line. Resistivity highs in

the field of high frequency between Nos.2 and 6, and Nos.9 and 12, correspond with the distribution of andesitic volcanics. Except the middle of the line, a stratiform geological structure is indicated by low resistivity measured with frequencies less than 128 Hz.

Line B. Distribution of resistivity is similar to that of Line A. High resistivity on high frequency is detected in the area of andesitic volcanics between Nos.8 and 10. Low resistivities of some 20 ohm-m are detected in the area of basalt in the west of the line.

Line C. Cuttings of stratiform contours are broadly found between No.5 and 8. The known fault is situated at No.8. Resistivity high is detected in the field of low frequency less than 256 Hz between Nos.5 and 6. Noticed is detection of low resistivity in the field of high frequency between Nos.8 and 12 in the east of the middle of the line, where volcanoclastic rocks are distributed. In the west of the line between Nos.0 and 4, where andesitic volcanics of high resistivity occur, low resistivities of less than 30 ohm-m are detected, probably due to thinness of volcanoclastic rocks.

Line D. The pattern of resistivity is similar to that of Line A. Discontinuance of stratiform contours is found between Nos.7 and 9. Resistivity high corresponding to andesitic volcanics is detected between Nos.0 and 5, with an indication of thickening of volcanoclastic rocks beneath Nos.2 and 3.

Line E. The pattern of resistivity is similar to that of Line D. Discontinuity of resistivity is seen at No.6 and No.8.

Line F. High resistivities in the field of high frequency are not a few in the middle of the line. Discontinuity of resistivity is recognized at Nos.4 and 7, but indistinct compared with those of Lines A to E.

Line G. Discontinuity of resistivity indicating an existence of fault is not found. In the field of high frequency, resistivity highs are detected in the west and in the eastern middle. The resistivity pattern of the line can be deemed to be similar to that of Line A.

Line H. A discontinuous contour pattern of resistivity is not recognized. In the middle of the line, high resistivity of a small scale is seen in the field of high frequency. A monotonous structure of resistivity is indicated.

In short, at the middle part of lines A to F, high resistivities of dike-shape are continuously detected which cut horizontal stratiform contours. This feature is apparent between Lines A and E, becomes smaller on Line F and disappears on Line G. Discontinuity of resistivity indicates fault(s). In the area of andesitic volcanics in the north, a fault is detected as a resistivity high in the field of high frequency.

(3) Maps of apparent resistivity

Figs.2-2-17 (1)-(3) show apparent resistivities on frequencies of 2,048 Hz, 256 Hz and 32 Hz, plotted on the scale of 1:10,000.

Map of 2,048 Hz. Fig.2-2-17 (1)

The map shows a specific character of resistivity at a shallow depth. Zones of high resistivity were

obtained at the northwest and the west of the area, probably due to an existence of andesitic volcanoclastic rocks. A small distribution of low resistivity is observed on the area of volcanoclastic rocks in the eastern middle of Line C, where alteration zone of mineral showing at Leli's prospect is known.

Map of 32 Hz. Fig.2-2-17 (3)

The map shows a specific character of resistivity at depths. Zones of low resistivities were broadly detected in the eastern half and in the northwest. These are assumed to correspond with volcanoclastic rocks, andesite, and basaltic andesite lava. In the western middle of Lines B to C, and Lines D to F, zones of high resistivity of more than 50 ohm-m are shown, trending toward north-south.

(4) Two-dimensional analysis

Figs.2-2-18 (1)-(2) show the results of two-dimensional analysis on all lines.

The central area is dominated by resistivity low, and zones of high resistivity are spread on Line A in the north and Lines G and H in the south, the north being of intrusive rocks and the south being of sheet-like spread such as basement rocks.

Compared with one-dimensional analysis, values of resistivity are lowered. The zone of high resistivity in the middle of lines in one-dimensional analysis is not seen on Lines B and C. Yet, the resistivity higher than that of surrounding area is noticed and a resistivity pattern similar to that of one-dimensional analysis has been obtained.

These results are summarized in Fig.2-5-19. Areas of zone of low resistivity less than 10 ohm-m and zone of high resistivity more than 50 ohm-m are shown, and discontinuity lines and the geological structure inferred from sections of apparent resistivity and from resistivity structural map are also shown in this Figure.

2-3-5 Results of Time Domain IP method

(1) Outline of the results

The time domain induced polarization method was conducted to clarify the relationships of geological structure and mineralization alteration with the zone of high resistivity delineated in the middle of Lines B to F of CSAMT method. Results are shown on sections of apparent resistivity in Fig.2-2-20 and on maps of Fig.2-2-21. Chargeability is also plotted on sections and maps as illustrated in Fig.2-2-22 and Fig.2-2-23.

(2) Apparent resistivity

The values of 15 to 25 ohm-m of apparent resistivity are dominant as those of CSAMT method. Consequently, criteria of high and low resistivity are placed at more than 50 ohm-m and less than 10 ohm-m.

Sections of apparent resistivity; Fig.2-2-20

Zones of low resistivity continuously extend in the east of each line. Also, resistivity highs detected in shallow depths of middle of Lines C to E are continuous. Other resistivity highs are detected in the west end of Lines E and F. These distributions accord with those of CSAMT method.

Maps of apparent resistivity; Figs.2-2-21 (1)-(5)

Five maps were provided with each electrode separation.

Map of $n=1$; Fig.2-2-21 (1)

Zones of high resistivity are detected in the middle of Lines B and C, and the western end of Lines E and F. The former is coincident at the trend of elongation and the scale of distribution with those of high resistivity zones detected by CSAMT method and assigned to be of alteration zone of silicification. The latter is in accord with distribution of andesitic volcanoclastic rocks. Moderate extent of resistivity low in the east of Lines A to E is correlative with distribution of volcanoclastic rocks, andesite and basaltic andesite lava.

Map of $n=2$; Fig.2-2-21 (2)

Values of zones of high resistivity on Lines C and D at $n=1$ are decreased in this map. An area of more than 50 ohm-m is of small scale between Nos.7 and 8 on Line E. The high resistivity zone at the western end of Lines E and F disappears. From this, layers of andesitic volcanoclastic rocks are assumed to be thin. In contrast, the zone of low resistivity is widespread.

Map of $n=3$; Fig.2-2-21 (3)

A zone of high resistivity is not seized at this separation. As for zones of low resistivity, the zone in the east of the area found at $n=1$ and $n=2$, is detected and the resistivity low of a small scale is newly located on Line E.

Map of $n=4$; Fig.2-2-21 (4)

The map has a distribution pattern of resistivity similar to that of map $n=3$. Only difference is seen with an existence of low resistivity of a small scale on Line A.

Map of $n=5$; Fig.2-2-21 (5)

A zone of low resistivity less than 10 ohm-m extends with a trend of northwest to southeast in the central part of the area. The zone appears to be increasing its extent toward southeast. The zone of low resistivity in the east of the area is divided into two directions of northwest and southeast.

(3) Chargeability

Dominant values of chargeability are less than $2 \text{ mV}\cdot\text{s}/\text{V}$, and values from $5 \text{ mV}\cdot\text{s}/\text{V}$ to $10 \text{ mV}\cdot\text{s}/\text{V}$ can be counted for weak anomalies, and values of more than $10 \text{ mV}\cdot\text{s}/\text{V}$ are counted for anomalies on chargeability.

Sections of chargeability; Fig.2-2-22

Weak anomalies more than $5 \text{ mV} \cdot \text{s/V}$ are successively detected in a northwest to southeast direction, at the western middle of each lines. These anomalies coincide with those seized by Geotrex in 1988, of which details are not known. Patterns of anomalies of each line are of pants-legs, which indicate a shallow origin of anomalies. Couples of negative and positive anomalies have been detected in depths between Nos.2 and 4 of Line C, between Nos.10 to 12 of Line D, and between Nos.6 to 10 of Line D. Anomalies are reproducible with data on $n=4$ to $n=5$ in depths, but their origins are unknown.

Maps of chargeability

Five maps were provided on each electrode separation.

Map of $n=1$; Fig.2-2-23 (1)

Weak anomalies of a northwest to southeast direction are distributed in the central part of the area. The location and the scale of anomalies coincides with the zone of high resistivity on the map of $n=1$ on apparent resistivity. Anomalous values are of the order of $5 \text{ mV} \cdot \text{s/V}$ and assumed to be of alteration zone of weak pyritization. Other weak anomalies of a small scale are also found at the eastern end of Line D and the western end of Line E. Negative anomalies are found at No.3 on Line B, No.3 on Line D and No.1 on Line F.

Map of $n=2$; Fig.2-2-23 (2)

The distribution of weak anomalies in the central part of the area has been transfigured. The anomalies spread on Lines C and D, and tend to reduce their extent on Lines B and E. Except the anomaly at the eastern end of Line D, weak anomalies and negative anomalies on the map of $n=1$ are not observed and a couple of negative and positive anomalies more than $10 \text{ mV} \cdot \text{s/V}$ is detected at the west end of Line C.

Map of $n=3$; Fig.2-2-23 (3)

The anomalies at the central part of the area are of reduced extent, and weak anomaly of a small scale and negative anomaly are detected in the middle of Lines E and F.

Map of $n=4$; Fig.2-2-23 (4)

Anomalies more than $10 \text{ mV} \cdot \text{s/V}$ are detected at Nos.2 and 3 of Line C, and zonal weak anomalies surround them in a north-northwest to south-southeast or north-south direction over an area from Line B to Line F. Weak or negative anomalies of a small scale are scattered in the east to the south of the area.

Map of $n=5$; Fig.2-2-23 (5)

High chargeability of $28.6 \text{ mV} \cdot \text{s/V}$ is detected at Nos.10 and 11 on Line D. Surrounding weak anomalies extend toward east of the middle of Lines D and E. Another weak anomaly spreads in the west of Lines B to D. Weak and negative anomalies appear alternatively in the middle of Lines E and F.

(4) Simulation of two-dimensional model

Values of resistivity and chargeability of each grid are set for the initial model with reference to the results of CSAMT analysis. Discrepancies occurred between measurements and the model on patterns and values of apparent resistivity, and setting of model is repeated with the method of trial and error to obtain a model of approximate values and contour patterns similar to the results of time domain induced polarization method.

Line B Fig.2-2-24 (1)

Modeling: Resistivity zone (code: 2) over 30 ohm-m is detected at the shallow part below the surface of stations between 5 and 7. The low resistivity zone (code: 3 and 6) is detected below of stations between 10 and 13. The weak chargeability anomaly over 5 mV·s/V (code :6) is detected at the deep part of stations between 3 and 6.

Results of simulation: The model brings the results most similar to apparent resistivity of the measurement. Chargeability also accords with the field data on the whole, but does not relate in detail, the negative anomaly at the shallow part below stations between 3 and 4, the part less than 3 mV·s/V between stations 6 and 7, and weak anomaly over 5 mV·s/V are not detected in the model.

Line C Fig.2-2-24 (2)

Modeling: The high resistivity zone (code: 4) at the shallow part below stations between 5 and 7 and the low resistivity zone (code: 1) are detected, and the “pants leg” pattern of chargeability anomaly (code: 4) below stations between 3 and 8 is measured. The pair of negative anomaly and zone over 10 mV·S/V is neglected because of limiting over the simulation.

Results of simulation: The sections of resistivity and chargeability show the results almost similar to the those of measurements, but are not simulated in detail. The distribution of origin of resistivity and chargeability on the whole are known.

Line E Fig.2-2-24 (3)

Modeling: The resistivity zone over 100 ohm-m at the west part of the survey line is coded by “6”. The high resistivity part shallow part below stations between 7 and 9 and charge-ability anomaly of the “pants leg” pattern below stations between 4 and 9 are coded by “4” and “5”.

Results of simulation The model shown in figure is brought the results most similar to resistivity and chargeability of the measurement.

The analytical results of TDIP method are summarized in Fig.2-2-25. The zone of low resistivity less than 10 ohm-m and of high resistivity more than 50 ohm-m are illustrated on the map of apparent resistivity. The location of the origin of anomalous chargeability and the geological structure obtained analytically by the simulation of two-dimensional model are also shown.

2-3-6 Laboratory Investigations

To know the resistivity and chargeability of rocks, samples were measured with the same instruments used in the field. Localities of thirty samples including drill-cores are shown in Fig.2-2-26. Rock samples comprise fifteen pieces of andesite, five of basalt, six of volcanoclastic rocks, and four of silicified rocks. Physical properties are listed in Table 2-2-3.

Table 2-2-3 Results of Physical Property of Rock Samples

No.	Rock	Resistivity (ohm-m)	Chargeability mVs/V	Remarks
1	Andesite	507	2.2	dark green, basaltic
2	Andesite	976	2.6	dark green, basaltic
3	Andesite	119	1.3	
4	Andesite	833	1.0	
5	Andesite	1098	2.4	
6	Andesite	1113	6.6	
7	Andesite	*92	*3.5	dark gray, weathered
8	Andesite	411	2.0	basaltic, porous
9	Andesite	2501	1.6	
10	Andesite	1272	2.3	
11	Andesite	1543	7.9	glassy
12	Andesite	514	4.6	porphyritic
13	Andesite	325	4.5	porphyritic
14	Andesite	471	8.4	porphyritic
15	Andesite	312	25.1	DDII-2 core 166m
	Average	857	4.8	
16	Basalt	*69	*1.7	green altered, porous
17	Basalt	1290	2.9	black
18	Basalt	489	2.5	black, with copper film
19	Basalt	2808	3.3	
20	Basalt	226	0.8	light gray, massive
	Average	1203	2.4	
21	Silicified rock	3911	2.3	dark gray, intensively
22	Silicified rock	1330	7.9	float, intensively
23	Silicified rock	2959	9.2	milky color, intensively
24	Silicified rock	3334	12.7	float
	Average	2884	8.0	
25	Volcanoclastic rock	28	6.8	andesitic breccia
26	Volcanoclastic rock	492	6.8	lapilli tuff
27	Volcanoclastic rock	281	12.3	white, altered
28	Volcanoclastic rock	116	2.9	pale green, basaltic
29	Volcanoclastic rock	37	12.2	
30	Volcanoclastic rock	313	29.0	light green, basaltic
	Average	211	11.7	

The distributions of resistivity and chargeability are illustrated in Fig.2-2-27.

The average resistivity and chargeability of andesite stand at 857 and 4.8 respectively, at 1203 and

2.4 of basalt, at 211 and 11.7 of volcanoclastic rocks, and at 2884 and 8.0 of silicified rocks.

The resistivity is highest in silicified rocks, and followed by basalt, andesite and volcanoclastic rocks in descending order. The values of silicified rocks are of about twice of resistivity in basalt, and basalt has some 50% higher values than those of andesite. The values of resistivity in volcanoclastic rocks are of a quarter of those of andesite.

The chargeability is highest in volcanoclastic rocks and followed by silicified rocks, andesite and basalt in descending order.

Distribution of resistivity in rocks is of scattered, and rocks have common ranges of resistivity values, as illustrated in Fig.2-2-27. Rocks cannot be specified from values of resistivity.

Chargeability has a distribution with small dispersion, and many samples show low values.

2-3-7 Summary of Geophysical Survey and Discussions

(1) Summary of array CSAMT survey

Results of CSAMT method are summarized as follows.

- a. The background value of apparent resistivity ranges from 15 to 25 ohm-m and low values are dominant on the whole.
- b. Zones of high resistivity more than 50 ohm-m are detected in shallow depths at the northwest and the west of the area, and inferred to be related with andesitic volcanoclastic rocks. Distribution of the zone of low resistivity is limited, with a small scale, only in the eastern middle of Line C where volcanoclastic rocks are dominated.
- c. Zones of low resistivity are widespread at the almost eastern half and the northwest of the area in depths, and inferred to be originated in volcanoclastic rocks, andesite and basaltic andesite lava. Zones of high resistivity more than 50 ohm-m are detected in the middle of Lines B to C, and Lines D to F.
- d. Zones of high resistivity of dike-shape, disturbing the horizontal contours of stratiform structure, are detected in sections of apparent resistivity at the middle of each line on Lines A to F. The phenomena are obvious on Lines A to E, diminish the scale at Line F and terminate on Line G.
- e. By the one-dimensional analysis of resistivity structure, the dyke-like zones of high resistivity are inferred to be of two bodies of high resistivity between Lines A to C and Lines D to F extending in a north-south direction. However, two bodies are deemed to form a zone that extends in a direction of northwest to southeast. The high resistivity originates probably in silicification because of its coincidence of distribution with that of silicified zone.

(2) Discussion on the results of array CSAMT survey

An outline of silicified alteration zone of Leli's mineral showing was revealed by CSAMT method that covered an area of the silicified zone and its vicinity. However, when more detailed survey is necessitated,

delineation of each silicified dyke becomes necessary. In case of this, it is considered that an electrode interval and spacing of survey line should be reduced to be of 25 to 50 m and 50 to 100 m respectively. With such specifications of investigation, more detailed mapping of resistivity becomes possible and it enables to analyze geological distribution and its structure in detail.

(3) Results of TDIP survey

Results of TDIP method are summarized as follows.

Resistivity

- a. Values of apparent resistivity are generally low and the background value ranges from 15 to 25 ohm-m.
- b. A zone of low resistivity less than 10 ohm-m has been detected successively between Nos.10 and 13 of each line, in a trend of north to south. Also, a zone of low resistivity has been found between Nos.6 and 8 in depth. Zones of low resistivity on small scales are known in shallow depths at the west of Lines A and C.
- c. Apparent resistivity of IP method is generally in accordance with distribution of apparent resistivity of CSAMT method, but values of apparent resistivity of the former tend to be lower than those of the latter.

Chargeability

- a. Values of chargeability in the background are of 2 to 3 mV·s/V, of which lower values predominate.
- b. Values of chargeability more than 10 mV·s/V have been obtained at three stations, No.3 on Line C, No.10 on Line 10 and No.7 on Line F. These are of isolated anomalies and of low reliability.
- c. A zone of higher values of chargeability more than 5 mV·s/V is detected in the depths between Nos.5 and 7 successively in a direction of northwest to southeast, and correlated to the IP anomalies found by Geotrex in 1988.
- d. The zone of high apparent resistivity delineated in the west of the middle of the area is situated at the almost same place where the concealed zone of high resistivity is found between Lines B to F by CSAMT method in a north-south trend. The concealed zone is assumed to be of silicified alteration zone. It is inferred that two methods revealed the same zone of high resistivity, and the area of weak anomaly on chargeability also coincides with the zone. From this, it is indicated that the silicified alteration is pyritized to some extent.
- e. Judging from the point of view on chargeability, intensive mineralization of sulfide minerals over a wide range is not expected in this area.

(4) Discussion on the results of TDIP survey

By TDIP method, the weak anomaly of chargeability more than 5 mV·s/V is detected at the west of the central area. The anomaly is the same with the IP anomaly revealed by Geotrex in 1988. Due to unavailability of previous data, absolute values of IP anomaly cannot be compared with those of present investigation. Yet, previous records revealed that line spacing and an electrode interval were of 40 m,

which enabled to make a detailed pursuit of anomalies.

In search of gold, the dipole-dipole induced polarization method is often confronted with a difficulty to detect the high resistivity of quartz veins or zones of silicification. More difficulties are expected when the zone is not accompanied with sulfide minerals. In case of this, the principal object should be rather placed to seize a zone of low resistivity caused from clayey alteration zone that is accompanied with the zone of silicification. Yet, due to the facts that the resistivity values of the background in this area are low, ranging from 15 to 25 ohm-m, and there exist the zone of low resistivity less than 10 ohm-m in the eastern half of the area, delineation of clayey alteration zone was difficult to be conducted.

2-4 Drilling

2-4-1 Method

(1) Location and length of drill holes

The locations, directions and lengths of the drill holes are listed below and shown in Fig.2-2-29 .

Table 2-2-4 Location, Orientation and Length of Drill Holes in the Dakuniba Area

Drill No.	Coordinates		Elevation (m)	Azimuth	Inclination	Drilled Length(m)
	Latitude	Longitude				
MJFV-1	16°32' 06"S	179°22' 27"E	100	S70°W	-45°	300.20
MJFV-2	16°32' 11"S	179°22' 29"E	50	S70°W	-45°	300.50
MJFV-3	16°32' 25"S	179°22' 36"E	40	S70°W	-45°	300.60

2-4-2 Drilling Method

(1) Transportation of machinery

The drilling equipment imported in the Radial warehouse in Suva and supplementary material stored in Suva were transported to the entrance of the drilling road near the Nakoroutari village by two trucks. The equipment was ferried from Natovi to Savusavu.

The rig and the compartment of pipes between drill sites were hauled by a Caterpillar D-6.

(2) Drilling Water

Water from nearby creeks was pumped up for drilling use. The pipe lengths for the drilling water and the pumped-up heights are as listed below.

Drill hole no.	Length of water supply pipe	Height from streams
MJFV-1	200 m	50 m
MJFV-2	300 m	20 m
MJFV-3	50 m	10 m

(3) Drilling program

A drilling rig of the Longyear L-44 was used. A PQ bit was used for drilling through the surficial weathered zone, reamed by PW casing shoe, and the PW casing pipes were inserted. For the whole length, except the surficial zone, wire-line method was used with PQ, HQ and NQ bits. Regarding loss of circulation which occurred during the operation, no special measures was taken and continued drilling to prevent the loss without significant disturbance.

Total core recovery was attempted. In cases where total recovery was not possible, at least 80% of the core was recovered.

(4) Drill Core Study

The recovered drill cores were studied in detail and 1:200 scale geologic columns were prepared.

Representative rocks were sectioned and studied microscopically, the mineralized parts were chemically analyzed and polished thin sections were studied. Constituent minerals were identified using X-ray diffraction analysis.

All the drill cores are stored in the MRD core shed near Labasa.

2-4-3 Geology, Mineralization and Alteration

(1) MJFV-1

The geology of the drill hole consists mainly of basalt lavas, basaltic andesite lavas and volcanoclastics of the Koroutari Andesites. The rocks is intruded by basaltic dykes(Fig 2-2-30). The drill hole encountered two mineralized zones.

① Geology

- 0-7.60 m : Soil.
- 7.60-38.20 m : Basalt lava. It shows amygdaloidal textures that are filled with quartz, zeolites and other minerals. The internal structure of the lava varies from autobrecciated one like hyaloclastite to massive compact one.
- 38.20-61.40 m : Lapilli tuff with intercalation of sandy tuff and tuff breccia. It shows grayish green and is rather soft. It is mainly composed of mafic lithic fragments. Weak grading is observed within 60 cm to 2 m. As the drill hole crosses bedding planes at about 75 degrees, the beds are estimated to dip about 30 degrees. A basalt dyke intrudes into the 38.90-39.20 m depth.
- 61.40-75.80 m : Basalt lava. It appears to be more compact than the basalt lava between 7.60 m and 38.20 m.
- 75.80-100.60 m : Coarse tuff, Lapilli tuff and tuff breccia. It shows brown or green color and is argillized intermittently and softened.
- 100.60-109.00 m : Basalt lava. It is massive and compact and shows dark green to black color.
- 100.90-120.80 m : Tuff breccia to lapilli tuff. It shows grayish green and widely brecciated and argillized. It is mainly composed of lithic fragments and hematitic cherty angular fragments. The interval between 120.10 m and 120.80 m is clay zone containing quartz breccia.
- 120.80-172.95 m : Basalt to basaltic andesite. It partly shows fine grained and appears to be intrusive.
- 172.95-176.53 m : Tuff breccia. It is composed of multi-colored lithic fragments and sandy matrix.
- 176.53-179.65 m : Basalt lava. It is compact and shows grayish green.
- 179.65-236.75 m : Tuff breccia. It is rather compact and massive. It is composed of basaltic to andesitic angular fragments of up to 10 cm of diameter. It partly contains scoria and shows agglomeratic texture .
- 236.75-245.60 m : Andesite lava. It shows grayish green and reddish, and compact porphyritic texture. It shows brecciated near the boundary of the lower unit (244.80-245.60 m).
- 245.60-300.20 m : Tuff breccia. It shows a texture similar to the rock between 179.65 m and 236.75 m.

② Mineralization and alteration

- 0-75.80 m : Weakly argillized. Smectite is identified by X-ray diffraction method. Neither pyritization nor other mineralization occurs. However, weak

silicification occurs at the depth of 11.20-12.00 m, weak argillization at the depth of 22.60-23.40 m and brecciation and argillization at the depths of 59.00-59.25 m, 60.80-61.40 m and 63.80-63.90 m.

- 75.80-120.45 m : Widely argillized. Pyrite dissemination is widespread. The intervals of 75.80-77.80 m, 82.80-83.60 m, 92.80-94.80 m and 118.50-120.80 m are stronger than other parts in terms of argillization and brecciation, and quartz veins occur. Especially, chlorite occurs between 120.0 m and 120.80 m. A sample from the quartz vein at 120.40-120.45 m depth assayed the value of 5.76 g/tAu.
- 120.80-232.20 m : Weak alteration turned the interval greenish. No pyrite dissemination is observed. Quartz-calcite veinlets occur at 155.8-158.8 m, 163.70-163.80 m, 166.70 m, 168.70 m, 171.30 m, 171.40 m, 174.70 m, 186.00 m, 195.10 m, 212.20 m, 222.00 m, 223.60 m, 229.25 m, 229.60 m and 231.00 m. No significant gold mineralization occurs (The assay value for the 0.30 m interval from the depth of 212.20 m is 0.011 g/tAu).

Depth(m)	Width (m)	Au (g/t)	Description
120.00-120.10	(0.10)	0.008	Clay zone
120.10-120.20	(0.10)	0.100	Quartz breccia zone
120.20-120.40	(0.20)	0.318	Quartz breccia
120.40-120.45	(0.05)	5.76	Quartz vein
120.45-120.80	(0.35)	0.404	Clay zone

- 232.20-300.20 m : Weakly silicified. Quartz - iron oxide veinlets and calcite veinlets occur. The veinlets occur most abundantly at the intervals of 236.00-250.65 m and 289.20-299.00 m. No significant gold mineralization is observed within these veinlets, as the assay value of the quartz vein at the depth of 256.00 m is 0.023 g/tAu over the 0.08 m interval.

(2) MJFV-2

The geologic units of the drill hole consist mainly of andesitic volcanoclastic rocks, basalt lavas, andesite lavas. A basaltic dyke intrudes at the depth of 72.10 m-85.80 m. The drill hole encountered two mineralized zones consisting of quartz - clay veins and a weakly silicified zone(Fig 2-2-31).

① Geology

- 0-9.85 m : Soil.
- 9.85-52.60 m : Lapilli tuff-coarse tuff. It shows mosaic texture consisting of mafic lithic fragments. The dip of the beds is estimated to be 30° since the hole crosses the beds at about 70° . The rock is weathered to the depth of 23.60 m and show brown to ochre color. The rock deeper than 23.60 m shows pale green. A fine tuff bed is intercalated at 51.70-52.60 m depth.
- 52.60-69.70 m : Volcanic conglomerate. It is composed of basaltic cobbles and boulders of 20 to 40 cm diameter and lapilli to ash size matrix. It is soft and pyrite is weakly disseminated. The matrix of the rock has been partly undergone oxidation and shows reddish.
- 69.70-72.10 m : Breccia zone. It is tectonically brecciated and weakly silicified. Pyrite dissemination and calcite veins occur.
- 72.10-85.80 m : Basalt dyke. It is hard and compact. It shows dark green. The texture is porphyritic and fine grained.
- 85.80-118.20 m : Scoria tuff-tuff breccia. It contains basaltic scorias at the depth of 85.80-94.30 m and shows brown and green. It is rather soft since it has been argillized to occur mixed-layer mineral. This zone may be a fault zone. The interval between 94.30 m and 118.75 m is tuff breccia, and consists of multi-color basaltic blocks and lapilli to fine ash size matrix.
- 118.20-118.75 m : Quartz vein within brecciated zone.
- 118.75-152.10 m : Basalt. It is fine grained and thought to be a intrusive rock. It shows dark green and is hard and compact. It contains olivine phenocrysts of 1-2 mm diameter. A thin bed of lapilli tuff is intercalated between the depths of 139.00 m and 139.05 m.
- 152.10-152.50 m : A thin bed of fine tuff.
- 152.50-159.65 m : Andesite lava. It is massive, compact and hard.
- 159.65-183.70 m : Tuff breccia. It comprises of green, red and black colored andesitic blocks and purplish matrix. The interval between 179.00 m and 182.50 m is autobrecciated. A bed of scoria tuff is intercalated between 182.50 m and 183.70 m.

- 183.70-198.00 m : Basaltic andesite lava. It shows green to red color and is hard. It is generally compact and unbrecciated, while the boundaries of two flow units at 183.70-186.00 m and 195.10-198.00 m are autobrecciated.
- 198.00-231.15 m : Tuff breccia. It consists of green, red and black colored andesitic breccia and more reddish matrix of ash. The percentage of blocks is more than the one of matrix.
- 231.15-251.30 m : Autobrecciated andesitic lava.
- 251.30-300.50 m : Tuff breccia. It may be termed agglomerate. It consists of andesitic breccia of 10-15cm diameter and matrix of same composition. It shows purplish green to red and hard. A thin bed of fine tuff is intercalated at the depth of 274 m. The intersected angle of the bed is about 45 degree and the dip of the bed is estimated to be about horizontal.

② Mineralization and alteration

- 9.85-72.10 m : Mixed-layer mineral and smectite occur and pyrite is disseminated weakly at this interval. The assay value for the interval of 53.30-54.70 m(1.40 m) is 0.031g/tAu.
- 72.10-118.20 m : It is weakly argillized to become greenish and has been undergone pyrite dissemination. Quartz veinlets and calcite veinlets occur at 74.15-74.35 m, 80.25 m and 97.00 m.
- 118.20-118.75 m : Quartz veining and brecciated zone. Assay values varies depending on the vein material as shown below. The average of three samples between 118.40 m and 118.75 m(0.35 m width) is 0.614g/tAu.

Depth (m)	Width(m)	Au (g/t)	Description
118.20-118.40	(0.20)	0.094	Quartz breccia, Green clay
118.40-118.45	(0.05)	0.890	Quartz
118.45-118.55	(0.10)	0.895	Stratified clay
118.55-118.70	(0.15)	0.254	Weakly brecciated zone
118.70-118.75	(0.05)	0.854	Weakly brecciated zone

- 118.75-232.20 m : Chloritization. Quartz hematite veins occur between 186.00 m and 195.60 m. A quartz vein between 195.10 m and 195.20 m (width 0.10 m) assays 0.010 g/tAu, and a quartz-iron oxide vein between 195.50 m and 195.60 m (width 0.10 m) 0.032g/tAu.

- 232.30-255.00 m : Weakly silicified. Quartz veinlets occur and assay low in gold: 0.010 g/tAu (245.45 m-246.45 m), and <0.008 g/tAu (250.45-250.57 m).
- 255.00 m-300.50 m : Chloritization. Calcite veinlets of 1 mm-5 mm width occur at many places. (A quartz vein occurs at the depth of 258.40 m.)

(3) MJFV-3

The geology of this hole consists of andesite lava, basaltic andesite lava and volcanoclastics of the Koroutari Andesites. Basaltic dykes intrude into this hole. Two gold mineralization zones occur and a weak silicification zone was encountered at depth (Fig.2-2-32).

① Geology

- 0-10.00 m : Soil.
- 10.00-19.70 m : Tuff breccia. It is basaltic andesitic and seems to be genetically autobrecciated. It is reddish due to oxidation.
- 19.70-32.80 m : Porphyritic basaltic andesite lava. It is dark green and autobrecciated.
- 32.80-36.90 m : Tuff breccia. It is dark green.
- 36.90-127.40 m : Basaltic andesite lava. It is autobrecciated and shows porphyritic texture. It is mostly dark green - pale green, and yellowish green.
- 127.40-131.70 m : Basalt dyke. It is dark green. It is medium grained and shows trachytic texture under microscopy. The boundary between the underlying tuff breccia is sharp and 70° .
- 131.70-151.60 m : It shows tuff breccia texture and appears to be genetically autobrecciated lava. It consists of pale green blocks and reddish ash matrix. A thin fine tuff layer is intercalated between 147.80 m and 148.40 m.
- 151.60-170.70 m : Tuff breccia. It consists of porphyritic andesitic lithic fragments and scoria matrix. It is massive. In some part lapilli size fragments are dominant.
- 170.70-180.70 m : Andesite lava. It appears to be more felsic than the lava at the upper units.
- 180.70-215.70 m : Tuff breccia. It consists of green andesitic angular blocks up to 20cm diameter and scoriaceous fragments with pale green and brown matrix of coarse ash.
- 215.70-221.90 m : Andesite lava. It is similar to the rock at the depth of 170.70-180.70 m. It is autobrecciated at the boundary with the lower unit.
- 221.90-244.60 m : Tuff breccia, lapilli tuff and tuff. It shows mosaic texture and multi-color and consists of andesitic blocks with minor amount basalt blocks of up to 70cm diameter. The content of the blocks is less than matrix content.

Scoriaceous fine tuffs and sandy tuffs are intercalated in the tuff breccias and lapilli tuffs.

- 244.60-262.20 m : Porphyritic basaltic andesite. It is compact and hard. It shows dark green and purplish green.
- 262.20-300.60 m : Alteration zone of volcanic breccia- tuff breccias and autobrecciated basaltic andesite lavas. The volcanic breccia- tuff breccia consists of scoriaceous sub-angular blocks and grayish green matrix. This interval includes lapilli tuff size parts. A basalt dyke intrudes into the depth between 295.00 m and 296.00 m.

② Mineralization and alteration

- 10.00-43.00 m : It is brown and soft due to the weak weathering. Smectite occurs. Pyrite dissemination is limited at the depth between 29.40 m and 29.70 m.
- 43.00-57.40 m : It shows greenish due to weak argillization(comprising of smectite). No pyritization occurs
- 57.40-77.80 m : Weakly argillized. Weak pyritization occurs. Gold mineralization is also weak as the most strongly argillized zone(67.40 m-67.55 m) assays 0.010g/tAu.
- 77.80-93.40 m : This zone is more weakly altered than the upper interval, and argillization is limited to fracture zones. Pyrite dissemination is also weak and limited.
- 93.40-131.70 m : Smectite and mixed-layer mineral occur and weak silicification is observed. Pyrite is disseminated weakly. The argillized zone including silicified volcanic blocks between 104.40 m and 104.90 m assays 0.638g/tAu.
- 131.70-155.80 m : Weakly argillized. The clay and breccia including quartz veining occur between 151.60 and 152.90 m. The interval between 152.10 m and 152.20 m(width 0.10 m) assays 5.06 g/tAu. Two samples from the apparent hanging wall and footwall assay 0.835 g/tAu(0.10 m) and 2.04 g/tAu(0.05 m), respectively.
- 155.80-177.60 m : Silicified. Hematite and quartz veinlets occur at 171.60 m-177.60 m. Mixed-layer mineral is identified by X-ray diffraction analysis. The 1.0 m intervals between 174.60 m and 175.60 m, and between 176.60 m and 177.60 m assay 0.014 g/t and 0.010 g/t, respectively.
- 177.60-244.60 m : Mixed-layer mineral is identified by X-ray diffraction analysis. No pyrite dissemination was observed. Calcite quartz veinlets occur at 210.90 m, 225.60 m and 226.60 m depths.
- 244.6-300.60 m : Weakly silicified. Calcite quartz veinlets occur. Chlorite and mixed-layer

mineral are identified from the samples within this interval. Quartz-calcite veins assay as low as 0.021 g/tAu (width 0.40 m), 0.012 g/tAu (width 0.13 m), 0.015 g/tAu (width 0.17 m).

2-4-4 Considerations on the Nakoroutari Area

(1) Summary of the drilling results

Geologic profiles and Schematic alteration zoning of the three holes are shown in Figs. 2-2-33 through -37. Three drill holes confirmed gold mineralization in quartz fragments - argillized zones (① and ②) hosted by the basalt and andesite lavas and volcaniclastic rocks. They also crossed a silicified zone (③). The significant zones are listed below:

(2) MJFV-1

① 60.80-77.80 m : The interval consists mainly of argillized zone with pyrite dissemination, and the following intervals were sampled for chemical analysis:

60.80-61.40 m Quartz argillized zone 0.029 g/tAu

75.80-77.80 m Quartz argillized zone <0.008 g/tAu

② 120.10-120.80 m : Argillized zone with pyrite dissemination. Major assay results are shown below:

120.20-120.40 m Argillized zone with quartz breccia 0.318g/tAu

120.40-120.45 m Argillized zone with quartz breccia 5.76g/tAu

(2) MJFV-2

① 118.20-118.75 m : Quartz breccia zone. The following interval was sampled for chemical analysis:

118.40-118.75 m (0.35 m) 0.614 g/tAu

② 186.00-195.60 m : Quartz-hematite veinlets zone. Neither wide quartz vein nor clay vein occurs in this interval. Even the most significant assays low in gold as follows:

195.50-195.60 m (0.10 m) 0.032g/tAu

③ 230-255 m : Silicified zone with quartz veinlets. One of the veinlets assays below 0.010 g/tAu.

(3) MJFV-3

① 57.40-77.80 m : Weakly argillized zone. The most strongly argillized zone assays 0.010 g/tAu.

93.40-119.20 m : Weakly brecciated zone

104.40-104.90 m : Silicified-argillized zone. The interval between 104.40 m and 104.90 m assays 0.638g/tAu.

② 151.90-152.60 m : Quartz breccia-argillized zone (galena and sphalerite occur.)

152.10-152.20 m (0.10 m) 5.06 g/tAu

152.20-152.25 m (0.05 m)

2.04 g/tAu

- ③ 245-256m : Calcite-quartz veinlets occur at the depth of 244.60-300.60 m. Especially, quartz veinlets occur in the silicified zone at 245-256m depth. The quartz veinlets assay low in gold and the highest value is 0.021 g/tAu.

In summary, gold mineralization occurs mainly in the two quartz breccia-argillized zones and one silicification zone. These zones trend in NNW-SSE direction and dip eastward. Namely, the quartz-argillized zone on the eastern side crosses MJFV-1 at 60.80 m-75.80 m depth, MJFV-2 near 118.20 m depth, and MJFV-3 near 67.40 m depth. The zone on the western side crosses the mineralized zone in MJFV-1 near 120.40 m depth, and MJFV-3 near 152.10 m depth, and it probably crosses MJFV-2 through the quartz angular fragments zone near 195 m depth, but mineralization is weaker than in the other two holes. Aside from the above two zones, a silicified zone is inferred to pass through the vicinity of 250 m depth of MJFV-2 and near 250 m depth of MJFV-3 with NNE-SSW strike. This silicified zone contains quartz veinlets.

(5) Characteristics of mineralization and structural control

a. Characteristics of mineralization

The mineralization accompanied by quartz angular fragments-silicified zones is of epithermal, and the lack or the paucity of sulfide minerals in the quartz veins and alteration zones is the characteristics of the mineralization of this area. The averages of homogenization temperatures of three quartz samples range from 200 to 270°C (Fig. 2-2-39), and the occurrence of chalcedonic quartz with crustified structure and other features indicate the shallow location of genesis. Regarding minor element content, however, although samples with high As and Hg content are harmonious with shallow genesis, As, Sb, and Hg contents are not necessarily high. It is seen that the Au/Ag ratio differs significantly among the high gold samples. Also electrum occurred in MJFV-3 and its Ag grade is low compared to Au content. The dominant gangue minerals are quartz and smectite with minor contents of adularia or carbonate minerals. It is noted that in the drill holes in this area, kaolin minerals and alunite are not observed, and enargite and luzonite are also absent. These facts indicate that this belongs to the low-sulfidation type gold mineralization (White and Hedenquist, 1990).

b. Alteration

The regional alteration of this area is generally weak. Chlorite-sericite and mixed-layer minerals were formed by hydrothermal alteration associated with mineralization, and these alteration zones are inferred to extend in the NW-SE direction with steep dip. Identification of the alteration minerals enabled the separation of the alteration zones of all the drill holes in this area into upper smectite zone and lower chlorite-sericite zone. And in MJFV-1, mixed-layer mineral occurs in between the smectite and sericite

zones and also below the chlorite-sericite zone. Although the detailed distribution of each alteration zone is not clear, chlorite-sericite zone extends in the NW-SE direction at steep dip. From this zoning of the alteration, it is considered that MJFV-1 and -3 penetrated the main part of the mineralization and alteration zones. Chlorite and sericite are believed to be the product of hydrothermal alteration associated with mineralization because mixed-layer mineral occurs again in the lower part of MJFV-1 and MJFV-3, and regional propylitization (chloritization) does not occur in this area.

c. Structural control on the mineralization

The mineralization of this area is concluded to be of low-sulfidation type controlled by the fracture system in basalt-andesite lava-volcaniclastic rocks. Mineralization of this type is a product of an extensive regional circulation of hydrothermal fluid, and the location of the heat source is not necessarily confined within the area. It may be necessary to consider a wider fluid circulation such as the that of the Labasa Caldera system. In fact, many hot springs occur in this caldera. During the first year survey, however, stronger mineralization has not been found outside of this Leli' Prospect area.

d. Re-interpretation of the geophysical investigation

Resistivity and chargeability were measured for the drill core samples(Fig.2-2-40). Thirty five samples are supplied for the measurement. The numbers of the samples for each rock type are 8 for andesite, 8 for basalt, 16 for volcaniclastic rocks and three for silicified-argillized rock. The average values of resistivity and chargeability classified by the rock types are:

- 255 ohm-m, 5.9 mV·s/V for andesite
- 155 ohm-m, 3.4 mV·s/V for basalt
- 146 ohm-m, 6.4 mV·s/V for volcaniclastic rocks
- 531 ohm-m, 6.3 mV·s/V for a silicified rock
- 33 ohm-m, 20.3 mV·s/V for argillized rocks.

The mineralization of this area has been concluded to be of low sulfidation type controlled by the fracture system in basalt-andesite lava-volcaniclastic rocks.

The weakly silicified zone where quartz veinlets occur is correlated to the CSAMT high resistivity anomaly under the Korobua Creek.

The IP anomaly that was estimated by a simulation extends to the deeper part of MJFV-2 and MJFV-3 (Figs. 2-2-41 and -42). The results of laboratory measurement of chargeability may not be high enough to explain the high chargeability of the simulation. The hematite and other iron oxides presence in silicified zone at depth may not be enough to produce the high anomaly since the volume of the iron oxides is limited. Consequently, pyrite dissemination at shallow depth is considered to be attributable to the anomaly.